PROTEIN STRUCTURE COMPARISON VIA CONTACT MAP ALIGNMENT

FELIPE LEAL VALENTIM

2010

FELIPE LEAL VALENTIM

PROTEIN STRUCTURE COMPARISON VIA CONTACT MAP ALIGNMENT

Dissertação apresentada à Universidade Federal de Lavras, como parte das exigências do Programa de Pós-Graduação em Biotecnologia Vegetal, área de Concentração em Biotecnologia Vegetal, para obtenção do título de "Mestre".

Orientador

Prof. Ricardo Martins de Abreu Silva

LAVRAS

MINAS GERAIS -BRASIL

2010

Ficha Catalográfica Preparada pela Divisão de Processos Técnicos da Biblioteca Central da UFLA

Valentim, Felipe Leal.
Protein Structure Comparison via Contact Map Alignment / Felipe Leal Valentim. – Lavras : UFLA, 2010.
77 p. : il.

Dissertação (mestrado) – Universidade Federal de Lavras, 2010.
Orientador: Ricardo Martins de Abreu Silva.
Bibliografia.

1. Proteínas. 2. Alinhamento estrutural. 3. Mapas de contato. 4. MAX-CMO. I. Universidade Federal de Lavras. II. Título.

CDD – 574.0285

FELIPE LEAL VALENTIM

PROTEIN STRUCTURE COMPARISON VIA CONTACT MAP ALIGNMENT

Dissertação apresentada à Universidade Federal de Lavras, como parte das exigências do Programa de Pós-Graduação em Biotecnologia Vegetal, area de Concentração em Biotecnologia Vegetal, para obtenção do título de "Mestre".

APROVADA em 05 de Fevereiro de 2010

Prof. Luciano Vilela Paiva - UFLA

Prof. Wagner Meira Junior - UFMG

Profa. Gloria Regina Franco - UFMG

Prof. Ricardo Martins de Abreu Silva
UFLA
(Orientador)

LAVRAS
MINAS GERAIS - BRASIL

SUMÁRIO

ABSTRACT

VALENTIM, Felipe Leal. **Protein Structure Comparison via Contact Map Alignment**. 2010. 77 p. Master thesis (Master in Plant Biotechnology) - Universidade Federal de Lavras, Lavras.*

Proteins are primary components in almost all biological processes in living organisms. It is known that the variety of protein functions is a result of the differences in protein structures. Therefore, understanding and comparing the structure of proteins is a major challenge in modern molecular biology. The structural alignment and comparison of proteins became an essential task, whose solution is instrumental in aiding other problems such as drug design, protein structure/function prediction, and protein clustering. One promising class of approaches for measuring protein similarity relies on the alignment of the protein contact maps. The most common mathematical statement of the contact map comparison problem is called the Maximum Contact Map Overlap (MAX-CMO). In this context, in this Master's thesis it has been proposed the hybrid heuristic Greedy Random Adaptive Search Procedure with Path-relinking for the Maximum Contact Map overlap problem which have been revealed able to find improved solutions. Another proposal which has been presented in this work is the implementation of a computational tool that allows the structural alignment of proteins through the proposed heuristic. The chapters 2 and 3 of this dissertation represent the manuscripts describing these two proposals and a final chapter that contains the conclusion and outlines the possibilities for future work.

Keywords: Proteins, Structural alignment, Contact Maps, MAX-CMO.

*__Advisor:__ Ricardo Martins de Abreu Silva - UFLA

RESUMO

VALENTIM, Felipe Leal. **Protein Structure Comparison via Contact Map Alignment**. 2010. 77 p. Dissertação (Mestrado em Biotecnologia Vegetal) - Universidade Federal de Lavras, Lavras.*

As proteínas são componentes primários em quase todos os processos biológicos nos organismos vivos. Sabe-se que a variedade de funções de proteínas é um resultado das diferenças nas estruturas de proteínas. Portanto, compreender e comparar a estrutura das proteínas é um desafio importante na biologia molecular moderna. O alinhamento estrutural e comparação das proteínas tornaram-se tarefas essenciais, cuja solução é fundamental para auxiliar outros problemas, tais como a desenho racional de novos fármacos, predição de função/estrutura de proteínas, e clusterização de proteínas. Uma classe promissora de abordagens para medir a similaridade da proteína depende do alinhamento dos mapas de contato da proteína. A fomalização mais comum para o problema matemático de alinhamento de mapas de contato é chamado o Maximum Contact Map Overlap problem (MAX-CMO). Neste contexto, esta dissertação de mestrado propõe a heurística híbrida Greedy Random Adaptive Search Procedure com Path-relinking para o Maximum Contact Map Overlap problem, que tem se revelado capaz de encontrar soluções promissoras. Outra proposta apresentada neste trabalho é a implementação de uma ferramenta computacional que permite o alinhamento estrutural de proteínas através da heurística proposta. Os capítulos 2 e 3 desta dissertação representam os artigos que descrevem estas duas propostas. Um capítulo final descreve experimentos adicionais realizados com a heurística e a ferramenta computacional.

Palavras-chave: Proteínas, Alinhamento estrutural, mapas de contato, MAX-CMO.

* **Orientador:** Ricardo Martins de Abreu Silva - UFLA

CHAPTER 1

GENERAL INTRODUCTION

1 PROTEIN STRUCTURES AND CONTACT MAPS

Proteins are primary components in almost all biological processes in living organisms. It is known that the variety of protein functions is a result of the differences in protein structures. Therefore, understanding and comparing the structure of proteins is a major challenge in modern molecular biology (Eidhammer et al., 2004).

Despite the large amount of diversity in their functions, all proteins are made of the same components, amino acids. And all amino acids share the same basic structure. Each amino acid consists of a central carbon atom (C_α), an amino group (NH_3), at one end, a carboxyl group ($COOH$) at the other end, and a side-chain (R) that characterizes the amino acids. This side-chain is usually referred to as an amino acid residue, or simply a *residue* (Eidhammer et al., 2004).

In order to form a protein molecule, the carboxyl group of one amino acid forms a peptide bond with the amino group of another amino acid and an (H_2O) molecule is revealed. The sequence of peptide bonds forms the protein backbone. There are 20 different side-chains specified by genetic code each of which is addressed by a letter of the alphabet. Since each protein is a sequence of amino acids, it can be described by a string over this set of 20 letters (Eidhammer et al., 2004).

The structure of proteins is organized in four structural levels: primary, secondary, tertiary, and quaternary structures. The linear sequence of amino acids that contribute to the formation of a protein molecule is called its primary structure. Many proteins contain roughly 100-1000 amino acids (Eidhammer et al., 2004) (some even more than 4000). Local arrangement of a few or a few dozen amino acid residues (Hunter, 1993) is seen in particular patterns repeatedly in many different proteins. These patterns are formed because of the interactions mediated by hydrogen bonds mainly within the backbone. The three-dimensional fold of the

protein molecule - which is a result of connecting secondary structures together - is called tertiary structure of the protein (Eidhammer et al., 2004). There are many proteins in nature which form from combinations of two or more protein chains. The spatial arrangement of these proteins is called *quaternary structure*. In this work, we are particularly interested in the tertiary structure of proteins, and when we refer to the protein structure in what follows, we will be referring to their tertiary ones.

1.1 Availability of structural data of proteins

The Protein Data Bank (PDB) (Berman et al., 2000) is the standard repository for collecting information on determined three-dimensional structures of proteins and other large biological molecules which are found in all of the living organisms. The coordinates of the structures in the PDB are determined by some experimental methods such as X-ray crystallography and Nuclear Magnetic Resonance (NMR) spectroscopy*. A rapid increase in the number of protein structures deposited in the PDB has been observed in recent years, and because of this growth, protein structure comparison has become a key problem in bioinformatics. This rapid growth has been related to the recent emergence of large scale protein structure determination projects (Nair et al., 2009), called structural genomics (Westbrook et al., 2003).

1.2 Protein Contact Maps

Three-dimensional structure of proteins can be represented by their *distance maps*. A distance map is an $N \times N$ matrix, where N is the number of amino acids in the sequence of a protein. Each element $d_{i,j}$ in the matrix D represents the distance between the i^{th} and the j^{th} amino acids, usually in Angestrom (Å). The distance between two residues can be defined in different ways, such as the

*More information about the PDB can be found in `http://www.wwpdb.org/documentation/`

distance between $C\alpha$ -$C\alpha$ (Vullo & Frasconi, 2003).

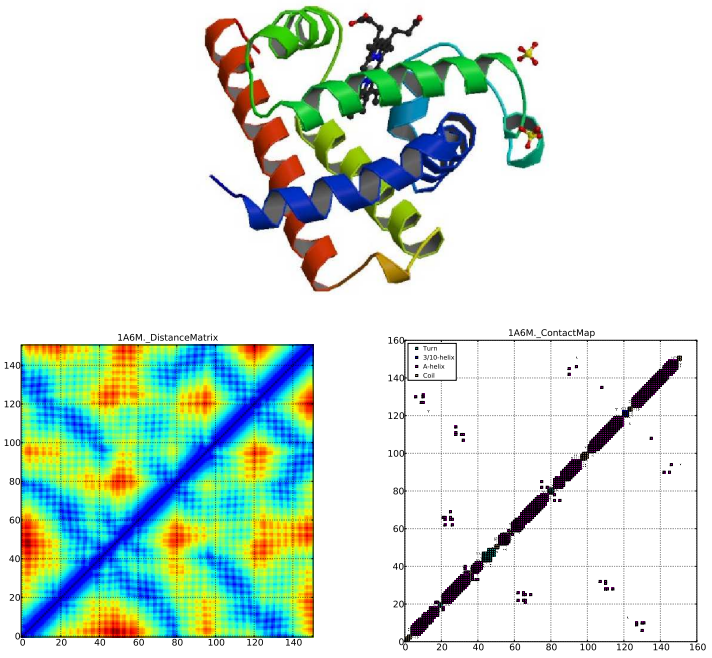

FIGURE 1 At the top, the protein PDB-ID:1am6 as taken from the PDB (Berman et al., 2000). On the left below, the extracted Distance Map of one chain of the protein. And on the right, Contact map of the same protein by applying the threshold of 6.5Å. Each pixel in this map indicates that the two corresponding amino acids are within the distance of 6.5Åof each other.

Contact maps are a thresholded version of distance maps. The contact map of a folded protein with N residues is a binary matrix $N \times N$ of all pairwise distances within that protein. Two residues are said to be *in contact* if the distance between their $C\alpha$ is not greater than a presumed threshold (typically in range 5Å-12Å) (Vullo & Frasconi, 2003) - see Figure 1.

Different secondary structures can be recognized in contact maps through their special patterns. In particular, α-helices appear as thick bands along the

main diagonal, while β-sheets appear as thin bands parallel or perpendicular to the main diagonal (Glasgow et al., 2006). Therefore, the contact map is a minimalist representation of a protein native three-dimensional structure (Krasnogor, 2004). This property leads to the idea that if two protein contact maps are similar to each other, their corresponding proteins have similar structures as well.

2 PROTEIN STRUCTURE COMPARISONS

Protein structure comparison has become a key problem in bioinformatics, improving researches that seek to find functional/evolutionary relationship among proteins and leading scientists in tasks such as protein function determination (Wolfon et al., 2005), rational drug (Wieman et al., 2004) design, the assessment of fold prediction (Goldsmith-Fischman & Honig, 2003), or protein clustering and classification (Dietmann et al.,2001). Moreover, structural alignment is a valuable tool for the comparison of proteins with low sequence similarity, where evolutionary relationships between proteins can not be easily detected by standard sequence alignment techniques (CAPRARA et al., 2000; Balaji & Srinivasan, 2007). A basic problem in pairwise protein structure comparison is finding a scoring scheme for similarity. Currently, most of the scoring schemes use the information about three-dimensional coordinates of protein structures, or their two-dimensional representations as distance maps. Another large class of approaches for measuring protein similarity relies on mutual comparison of contact maps. These methods are based on the hypothesis that similarity in protein contact maps results in similarity in protein structures. In this work, we focus on this approach of alignment of contact maps.

2.1 Contact Map Alignment

A large class of methods for protein structure comparison scores the similarity of proteins by comparing their binary contact maps. These approaches are based on the hypothesis that contact maps capture important information about the native structure of proteins (Krasnogor et al., 2003). Thus, the similarity between contact maps results in similarity between protein structures. The most common mathematical statement of the contact map comparison problem is called the *Maximum Contact Map Overlap* (Greenberg et al., 2004) (MAX-CMO). In the formulation of this problem, contact maps are interpreted as adjacency matrices of graphs. Each protein is represented by a graph whose nodes correspond to one of the amino acids of that protein. There is an edge between two nodes of the graph whenever their corresponding amino acids are in contact, i.e., their positions in the three-dimensional structure of the protein are within a specified distance of one another. The problem is now to calculate the similarity of proteins by aligning the two contact map graphs. The alignment value (i.e. the amount of similarity) is determined by the size of the common subgraph, which is identified by the alignment, that is, the number of edges connecting two equivalent nodes in both graphs. Chapter 2 details this problem.

3 OBJECTIVES AND STRUCTURE OF THE THESIS

This project main objective, which proposal is detailed in Chapter 2, is the development of a novel and efficient heuristic for the Maximum Contact Map Overlap problem. The chapter 2 represents the manuscript describing this proposal - introduction, review, formalizations and mathematical modeling of the MAX-CMO problem; methodology development; our proposal presented as the GRASP-PR algorithm for the MAX-CMO problem; as well as presenting the

results of performed analyses. This manuscript meets the requirements of the journal “IEEE/ACM Transactions on Computational Biology and Bioinformatics” (TCBB) for publishing an article of type “Regular Paper”.

A secondary objective – presented in Chapter 3 as a brief manuscript – is the implementation of a computational tool that allows the structural alignment of proteins through the proposed heuristic and also other successful algorithms described in subsequent chapters. This second manuscript meets the requirements and restrictions of the journal “Bioinformatics” (Oxford journals) to publish an article of type ”Application Note”.

The fourth and final Chapter contains the conclusion and outlines the possibilities for future work.

4 REFERENCES

BALAJI, S.; SRINIVASAN, N. Comparison of sequence-based and structurebased phylogenetic trees of homologous proteins: inferences on protein evolution. **Journal of Biosciences**, Bangalore, v. 32, n. 1, p. 83–96, Jan. 2007.

BERMAN, H. M.; WESTBROOK, J.; FENG, Z.; GILLILAND, G.; BHAT, T. N.; WEISSIG, H.; SHINDYALOV, I. N.; BOURNE, P. E. The protein data bank. **Nucleic Acids Research**, Oxford, v. 28, n. 1, p. 235–242, Jan. 2000.

CAPRARA, A.; CARR, R.; ISTRAIL, S.; LANCIA, G.; WALENZ, B. 1001 optimal pdb structure alignments: integer programming methods for finding the maximum contact map overlap. **Journal of Computational Biology**, New York, v. 11, n. 1, p. 27–52, Jan. 2004.

DIETMANN, S.; PARK, J.; NOTREDAME, C.; HEGER, A.; LAPPE, M.; HOLM, L. A fully automatic evolutionary classification of protein folds: dali domain dictionary version 3. **Nucleic Acids Research**, Oxford, v. 29, n. 1, p. 55–57, Jan. 2001.

EIDHAMMER, I.; JONASSEN, I.; TAYLOR, W. R. **Protein bioinformatics**: an algorithmic approach to sequence and structure analysis. New York: J. Wiley, 2004.

GLASGOW, J.; KUO, T.; DAVIES, J. Protein structure from contact maps: a case-based reasoning approach. **Information Systems Frontiers**, Boston, v. 8, n. 1, p. 29–36, Feb. 2006.

GOLDSMITH-FISCHMAN, S.; HONIG, B. Structural genomics: computational methods for structure analysis. **Protein Science**, Cold Spring Harbor, v. 12, n. 9, p. 1813–1821, Sept. 2003.

GREENBERG, H. J.; HART, W. E.; LANCIA, G. Opportunities for combinatorial optimization in computational biology. **Informs Journal on Computing**, Linthicum, v. 16, n. 3, p. 211–231, 2004.

HUNTER, L. Artificial intelligence & molecular biology. **Al Magazine**, Menlo Park, v. 11, n. 4, p. 1–46, 1993.

KRASNOGOR, N. Self generating metaheuristics in bioinformatics: the proteins structure comparison case. **Genetic Programming and Evolvable Machines**, Dordrecht, v. 5, n. 2, p. 181–201, June 2004.

KRASNOGOR, N.; LANCIA, G.; ZEMLA, A.; HART, W. E.; CARR, R. D.; HIRST, J.; BURKE, E. A comparison of computational methods for the maximum contact map overlap of protein Pairs. 2003. Available at: <http://citeseerx.ist.psu.edu/viewdoc/summary?doi=10.1.1.3.4526>. Accessed: 3 dez. 2009.

NAIR, R.; LIU, J.; SOONG, T. T.; ACTON, T. B.; EVERETT, J. K.; KOURANOV, A.; FISER, A.; GODZIK, A.; JAROSZEWSKI, L.; ORENGO, C.; MONTELIONE, G. T.; ROST, B. Structural genomics is the largest contributor of novel structural leverage. **Journal of Molecular Biology**, London, v. 10, n. 2, p. 181–191, Apr. 2009.

VULLO, A.; FRASCONI, P. Prediction of protein coarse contact maps. **Journal of bioinformatics and computational biology**, London, 1, n. 2, p. 411–431, July 2003.

WESTBROOK, J.; FENG, Z.; CHEN, L.; YANG, H.; BERMAN, H. M. The protein data bank and structural genomics. **Nucleic Acids Research**, Oxford, v. 31, n. 1, p. 489–491, 2003.

WIEMAN, H.; TONDEL, K.; ANDERSSEN, E.; DRABLOS, F. Homology-based modelling of targets for rational drug design. **Mini-Reviews in Medicinal Chemistry**, Hilversum, v. 4, n. 7, p. 793–804, Sept. 2004.

WOLFON, H. J.; SHATSKY, M.; SCHNEIDMAN-DUHOVNY, D.; DROR, O.; SHULMAN-PELEG, A.; MA, B.; NUSSINOV, R. From structure to function: methods and applications. **Current Protein and Peptide Science**, Amsterdam, v. 6, n. 2, p. 171–183, Apr. 2005.

CHAPTER 2

GRASP WITH PATH-RELINKING FOR THE MAXIMUM CONTACT MAP OVERLAP PROBLEM

1 ABSTRACT

Structural alignment emerged as a valuable tool for the comparison of proteins with low sequence similarity, since structurally similar but sequentially unrelated proteins have been discovered and rediscovered by many researchers. Recently, the growth of the Protein Data Bank has been accelerated by a large scale structure determination projects, and thus, fast and efficient algorithms for protein structure comparison has become more important to take advantage of the huge amount of structural data. There exist several approaches to perform the structural alignment, being the solution of the Maximum Contact Map Overlap problem one efficient available alternative. Although Maximum Contact Map Overlap problem may be solved using exact algorithms, simple approximate algorithms that obtains good quality solutions using less computational resources and time are still required. This paper proposes a variant of the greedy randomized adaptive search procedure with path-relinking (GRASP-PR) for MAX-CMO. Computational experiments are performed comparing a GRASP-PR heuristic with other algorithms from literature on real and simulated data. The GRASP-PR heuristic effectiveness is analyzed, demonstrating that our approach is a promising strategy to resolve the problem.

Keywords: Structural alignment, maximum contact map overlap problem, GRASP with Path-Relinking.

2 RESUMO

O alinhamento estrutural emergiu como uma valiosa ferramenta para comparação de proteínas com baixa similaridade de seqüência, visto que proteínas com estruturas semelhantes mas seqüencialmente não relacionadas têm sido descobertas e redescobertas por muitos pesquisadores. Recentemente, o crescimento do banco de dados da proteínas foi acelerado por uma grande escala de projetos de determinação estrutural e, assim, algoritmos rápidos e eficientes para a comparação da estrutura da proteína têm se tornado mais importantes para tomarem vantagem sobre a enorme quantidade de dados estruturais. Existem diversas abordagens para realizar o alinhamento estrutural, sendo a solução do *Maximum Contact Map Overlap problem* uma eficiente alternativa disponível. Embora o *Maximum Contact Map Overlap problem* possa ser resolvido utilizando algoritmos exatos, simples algoritmos aproximados que obtêm soluções de boa qualidade utilizando menos recursos computacionais e tempo continuam necessários. Este artigo propõe uma variação da *heurística greedy randomized adaptive search procedure* com *path-relinking* (GRASP-PR) para o MAX-CMO. Experimentos computacionais são realizados comparando o GRASP-PR contra outros algoritmos da literatura em dados simulados e reais. A eficiência da heurística GRASP-PR é analizada, demonstrando que nossa proposta é uma estratégia promissora para resolver o problema.

Palavras-chave: Alinhamento estrutural, *maximum contact map overlap problem*, *Greedy Random Adaptive Search Procedure* com *Path-relinking*.

3 INTRODUTION

Proteins are organic compounds that play an important role in nearly all cell processes, including metabolic, immunological, cell signaling, and regulation of the cell cycle. Proteins are made up of amino acids arranged in a linear chain and folded in a three dimensional form. An amino acid is a molecule containing an amino group, a carboxyl group, and a side chain usually referred to as an amino acid residue, or simply a *residue*. One can think of a protein as being made up of a backbone with hanging residues (see Figure 1). Note that although two residues may be far apart in the backbone, because of the three dimensional form of the protein, they may actually be close together. From the 20 standard amino acid building blocks, perhaps millions of proteins exist in nature, most of which currently have unknown function.

Protein structure alignment has become a standard structural analysis tool analysis tool providing similarity measures between the structures. Protein structure similarity may indicate functional/evolutionary relationship that usually leads scientists in tasks such as protein function determination (Wolfson et al., 2005), rational drug (Wieman et al., 2004) design , assessment of fold (Goldsmith-Fischman & Honig, 2003) prediction or protein clustering and classification (Dietmann et al., 2001). Recently, the growth of the Protein Data Bank (PDB) (Berman et al., 2000) has been accelerated by a large scale structure determination projects, called *structural genomics* (Westbrook et al., 2003). As a result, fast and efficient algorithms for protein structure comparison have become more important to take advantage of the huge amount of structural data.

One promising way of accomplishing the structural alignment is to evaluate the alignment of their contact maps. A *protein contact map* is used to represent the distances between every pair of residues in a three-dimensional protein structure.

The distance between two residues is usually defined as being either the smallest Euclidean distance between the points where the two residues connect to the backbone structure or as the smallest Euclidean distance between any pair of atoms in the residues.

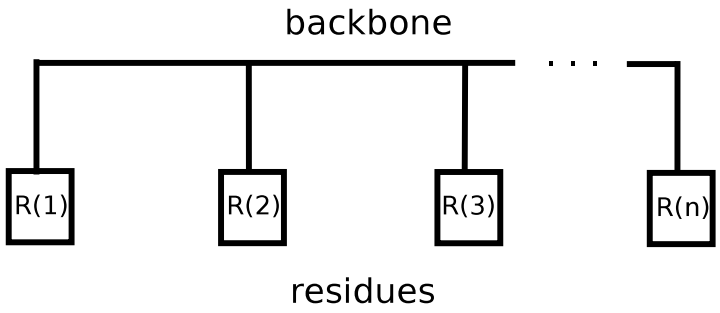

FIGURE 1 A protein can be viewed as a chain of hanging residues.

A contact map (see Figure 2) consists of either a graph or a two-dimensional matrix (binary or real). The graph representation (Figure 2.c) shows the contact map as a graph with a sequence of nodes corresponding to the sequence of residues and an edge for each pair of non-consecutive residues whose distance is below a given threshold. The *length* of a contact map in the graph representation is defined by the number of nodes in the graph.

For a protein with n residues $\{1, 2, \ldots, n\}$, the binary matrix representation (Figure 2.a) is a square $(0, 1)$ $n \times n$ matrix C where the element $C_{i,j}$, for $i, j = 1, \ldots, n$ $(i \neq j)$, indicates whether the distance δ_{ij} between non-consecutive residues i and j is less than a predefined distance threshold t, i.e.

$$C_{i,j} = \begin{cases} 1 & \text{if } \delta_{ij} < t \text{ and } |j - i| > 1; \\ 0 & \text{otherwise.} \end{cases}$$

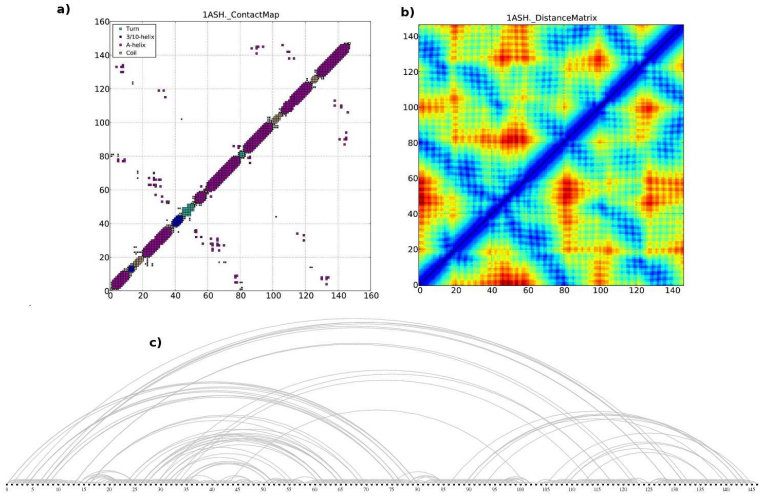

FIGURE 2 Three contact map representations of protein PDB-ID:1ash: (a) as binary matrix, (b) as a real matrix (distance map), and (c) as a graph. The interested reader is referred to (Ho et al., 2008) for a detailed description of the generation of contact maps.

With respect to the real matrix representation (shown in Figure 2.b), a contact map is a square real-valued matrix C, where $C_{i,j} = \delta_{ij}$.

Contact maps provide a more compact representation of the protein structure than its corresponding three dimensional atomic coordinates. The advantage is that contact maps are invariant to rotations and translations, both favorable properties for the comparison of protein structures. For more detail, the reader is referred to (Bartoli et al., 2008). In the remainder of this paper, we restrict our attention to the contact map graph representation. The terms *nodes* in a contact map and *residues* in a protein will be interchangeable.

To determine the similarity of two proteins requires the definition of a metric. In this paper we use two similarity metrics. This first, called *contact map overlap* (Goldman et al., 1999) is illustrated in Figure 3. This figure is derived from a

similar figure in (Lancia et al., 2001). The alignment shows the residues selected in the subgraphs (nodes 1, 2, 4, 5, 6, 7, and 8 from V_A and nodes 1, 2, 3, 5, 7, 9, and 10 from V_B). The linear ordering is preserved by associating $1 \leftrightarrow 1$, $2 \leftrightarrow 2$, $4 \leftrightarrow 3$, $5 \leftrightarrow 5$, $6 \leftrightarrow 7$, $7 \leftrightarrow 9$, and $8 \leftrightarrow 10$. The corresponding edges in the isomorphic graphs are solid and color matched. These edges satisfy the condition that their endpoints are associated. For example, edge $(1, 4)$ in E_A corresponds to edge $(1, 3)$ in E_B because of node associations $1 \leftrightarrow 1$ and $4 \leftrightarrow 3$.

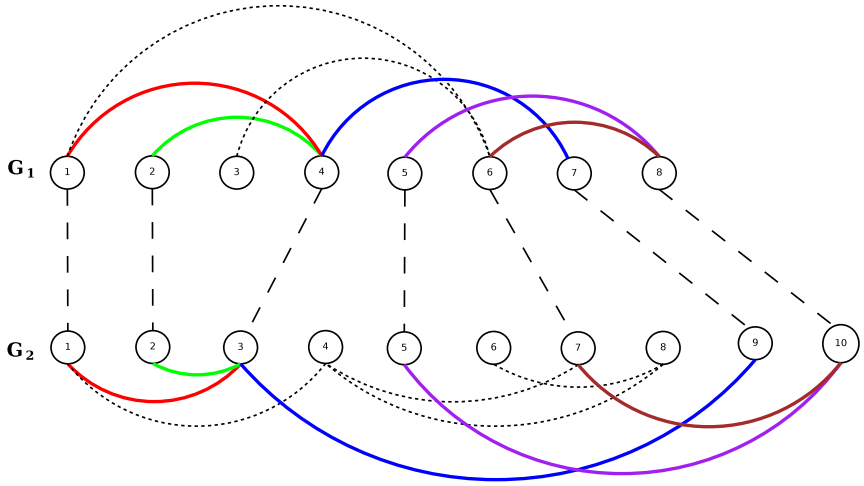

FIGURE 3 Example of contact map alignment. Isomorphic subgraphs have five (solid color-matched) edges each (Lancia et al., 2001).

Figure 4 shows an optimal alignment (overlapped edges are identified by red lines) between the contact maps for distinct proteins *1hlm*[*] (Figure 4.a) and *1ahs*[†] (Figure 4.b). The alignment value is defined as the number of edges of each subgraph identified by the alignment, i.e., the set of corresponding edges in each graph.

[*] `http://www.rcsb.org/pdb/explore/expore.do?structureId=1HLM`
[†] `http://www.rcsb.org/pdb/explore/expore.do?structureId=1AHS`

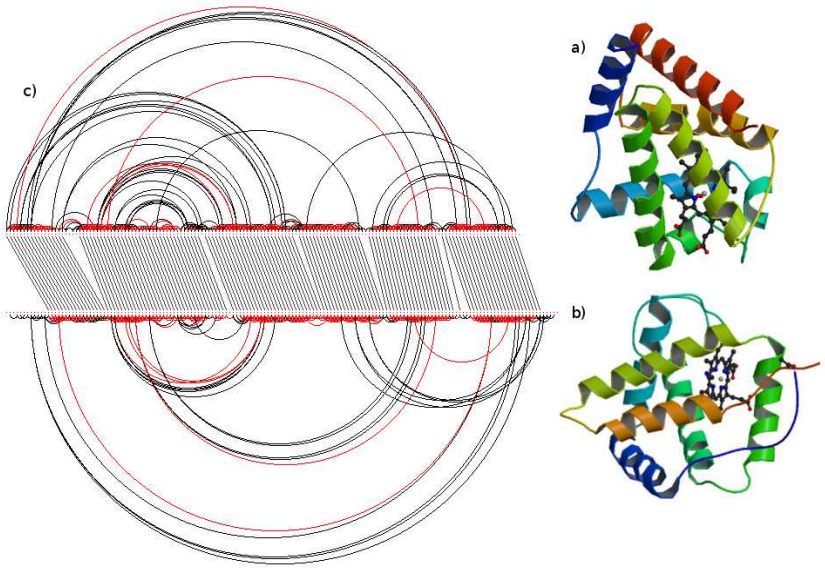

FIGURE 4 Three dimensional native structures for proteins (a) *1ash* and (b) *1hlm* as taken from the Protein Data Bank (PDB) (Berman et al., 2000), and (c) an optimal alignment of value 279 of two 6.5Å threshold contact maps of the proteins. The optimal value was determined in (Xie & Sahinidis, 2007) with a branch and bound algorithm. This alignment was generated with a pure GRASP (without path-relinking) heuristic. The figure was created with a modified version of the java program `BuildContactMapFromPDB` available at `http://www.cs.nott.ac.uk/~nxk/USM/protocol.html`.

Given two contact maps $G_A = (V_A, E_A)$ and $G_B = (V_B, E_B)$ such that $|V_A| = n$ and $|V_B| = m$, the CONTACT MAP OVERLAP PROBLEM (Goldman et al., 1999) is to find two subsets $S_A \subseteq V_A$ and $S_B \subseteq V_B$ with $|S_A| = |S_B|$ and an order preserving bijection f between S_A and S_B such that the cardinality of the *overlap set*

$$\mathcal{L}(S_A, S_B, f) = \{(u, v) \in E_A \ : \ u, v \in S_A, \ (f(u), f(v)) \in E_B\}$$

is maximized. A solution (S_A, S_B, f) for the contact map overlap problem can be represented as an assignment vector p of size n such that

$$p_u = \begin{cases} v & \text{if } (u, v) \in \mathcal{L}(S_A, S_B, f) \\ \texttt{nil} & \text{otherwise.} \end{cases}$$

We later refer to the cardinality $|\mathcal{L}(S_A, S_B, f)|$ of the overlap set defined by p as $\Lambda(p)$.

The contact map overlap problem was shown by (Goldman et al., 1999) to be NP-hard and can be formulated as a $(0, 1)$ integer program (Greenberg et al., 2004). Define the binary variable $x_{ij} = 1$ if and only if node $i \in V_A$ is associated with node $j \in V_B$, and define the binary variable $y_{(i,k)(j,l)} = 1$ if and only if $(i, k) \in E_A$ and $(j, l) \in E_B$ are corresponding edges in the isomorphic subgraphs. The objective of the CMO problem is to maximize

$$\sum_{\substack{(i,k)\in E_A \\ (j,l)\in E_B}} y_{(i,k)(j,l)}.$$

The selected edges must have their endpoints associated in such a way that

$$y_{(i,k)(j,l)} = 1 \Rightarrow x_{ij} = x_{kl} = 1,$$

i.e.

$$y_{(i,k)(j,l)} \leq x_{ij},$$
$$y_{(i,k)(j,l)} \leq x_{kl},$$

for all $(i, k) \in E_A$ and $(j, l) \in E_B$. Furthermore, at most one node in one graph

can be associated with a node in the other graph, i.e.:

$$\sum_{i \in V_A} x_{ij} \leq 1, \forall j \in V_B,$$
$$\sum_{j \in V_B} x_{ij} \leq 1, \forall i \in V_A.$$

Finally, any two associations (edges with one endpoint in V_A and the other in V_B) cannot cross, i.e.:

$$x_{ij} + x_{kl} \leq 1, \quad \text{for } 1 \leq i < k \leq |V_A| \text{ and } 1 \leq l < j \leq |V_B|.$$

The second similarity measure used in this paper is the *root mean square deviation* (RMSD). This measure is not used directly in our heuristic. Instead, it is used only to verify the quality of the solutions found by the heuristic. The RMSD is the average distance between the backbones of superimposed proteins. We use the tool `Biopython` of (Cock et al., 2009) to compute the RMSD values.

The contact map overlap problem was introduced in (Godzik et al., 1992). Several exact algorithms as well as heuristics have been since proposed for this problem. (Lancia et al., 2001) describe a branch and cut strategy that employs lower-bounding heuristics at the branch nodes. (Caprara & Lancia, 2002) proposed a Lagrangian relaxation approach, where the optimal Lagrange multipliers are found by subgradient optimization. (Carr et al., 2002) proposed a memetic evolutionary algorithm. (Xie & Sahinidis, 2007) used dynamic programming as tool to design a branch-and-bound algorithm with several reduction techniques to eliminate inferior residue-residue pairs early in the search procedure. (Pelta et al., 2008) proposed three versions of a multi-start variable neighborhood search heuristic for solving MAX-CMO.

The remainder of the paper is organized as follows. In Section 4 we present the GRASP with path-relinking heuristic for the MAX-CMO problem. Computational experiments are described in Section 5.2. Finally, concluding remarks are made in Section 6.

4 GRASP WITH PATH-RELINKING FOR MAX-CMO

A GRASP heuristic (Feo & Resende, 1995; Resende & Ribeiro, 2003) is a multi-start procedure in which a greedy randomized solution is constructed to be used as a starting solution for local search for all iterations. Local search repeatedly substitutes the current solution by a better solution in the neighborhood of the current solution. If there is no better solution in the neighborhood, the current solution is declared a local maximum and the search stops. The best local maximum found over all GRASP iterations is output as the solution.

GRASP iterations are independent, i.e. solutions found in previous GRASP iterations do not influence the algorithm in the current iteration. The use of previously found solutions to influence the procedure in the current iteration can be thought of as a memory mechanism.

One way to incorporate memory into GRASP is with path-relinking (Glover, 1996). In GRASP with path-relinking (Laguna & Martí, 1999; Resende & Ribeiro, 2005), an elite set of diverse good-quality solutions is maintained to be used in all GRASP iterations. After a solution is produced with greedy randomized construction and local search, that solution is combined with a randomly selected solution from the elite set using the path-relinking operator. The combined solution is then considered apt to be included in the elite set. Ultimately, it is added to the elite set if it meets quality and diversity criteria.

```
procedure GRASP+PR-CMOP
  Input: C^A, C^B
  Output: solution p*
P ← ∅;
while stopping criterion not satisfied do
    p ← GreedyRandomized(·);
    p ← ApproximateLocalSearch(p);
    if P is full then
        Randomly select a solution q ∈ P;
        r ← PathRelinking(p, q);
        r ← ApproximateLocalSearch(r);
        if c(r) > max{c(s) : s ∈ P} then
            t ← argmin{Δ(r, s) : s ∈ P};
            P ← P ∪ {r} \ {t};
        else if c(r) > min{c(s) : s ∈ P} and r ≉ P then
            t ← argmin{Δ(r, s) : s ∈ P : c(s) < c(r)};
            P ← P ∪ {r} \ {t};
        end
    else
        if P = ∅ then
            P ← {p};
        else if p ≉ P then
            P ← P ∪ {p};
        end
    end
end
return p* = argmax{c(s) : s ∈ P};
```

Algorithm 1: Pseudo-code of the GRASP-PR heuristic for MAX-CMO.

Algorithm 1 shows pseudo-code for the GRASP with path-relinking heuristic for the MAX-CMO problem. The algorithm takes two contact maps as input C^A and C^B of proteins A and B, with n and m residues ($m > n$), respectively. It outputs an array p^* of length n, with $p_i^* = \texttt{nil}$, if node $i \in C^A$ representing residue $i \in A$ is not aligned, and $p_i^* = j$, if node $i \in C^A$ is aligned with node $j \in C^B$.

After initializing the elite set P as empty in line 1, the GRASP with path-relinking iterations are computed in lines 2 to 26 until a stopping criterion is satisfied. This criterion could be, for example, a maximum number of iterations, a target solution quality, or a maximum number of iterations without improvement. During all iterations, a greedy randomized solution p is generated in line 3 and tentatively improved in line 4 with an approximate local search. The greedy randomized construction and the approximate local search are described in Subsections 4.1 and 4.2, respectively.

If the elite set P is empty, solution p is added to it in line 20. If the elite set is not empty, then while it is not full, solution p is added to it in line 23 if it is sufficiently different from the solutions already in the elite set. To define the term "sufficiently different" more precisely, let $\Delta(p, q)$ denote the number of assignments in p that are different from those in q. For a given level of difference δ, we say p is sufficiently different from all elite solutions in P if $\Delta(p, q) > \delta$ for all $q \in P$, which we indicate with the notation $p \not\approx P$.

If the elite set P is full, then path-relinking is applied in line 7 between p and some elite solution q randomly chosen from P in line 6, resulting in solution r. In line 8, r is updated by an approximate local minimum in its neighborhood. Path-relinking is described in Subsection 4.3.

If r is the best solution found so far, then in line 11 it replaces t, the solution

most similar to it, computed in line 10. Otherwise, if r is better than the worst solution in P and $r \not\approx P$, then in line 15 it replaces t, the solution most similar to it, computed in line 14.

4.1 Greedy randomized construction

Greedy randomized construction in a GRASP heuristic combines elements of a greedy algorithm with randomization to produce a series of starting solutions for local search. Pseudo-code for the greedy randomized procedure for the MAX-CMO problem is shown in Algorithm 2, referred to in line 3 of Algorithm 1 as `GreedyRandomized`.

procedure `GreedyRandomized`
  Input: $C^A = (V_A, E_A)$, $C^B = (V_B, E_B)$, α
  Output: Assignment vector p
1 Randomly select $q \in$ UNIF$[\lceil \alpha \times n \rceil, n]$;
2 Initialize $R^A \leftarrow \emptyset$; $R^B \leftarrow \emptyset$;
3 **for** $i = 1, \ldots, q$ **do**
4 | Randomly select $r_A \in V_A$ with $\text{prob}(r_A) \sim \deg(r_A)$;
5 | $R^A \leftarrow R^A \cup \{r_A\}$;
6 | Randomly select $r_B \in V_B$ with $\text{prob}(r_B) \sim \deg(r_B)$;
7 | $R^B \leftarrow R^B \cup \{r_B\}$;
8 **end**
9 Sort R^A and R^B in increasing order;
10 **for** $k = 1, \ldots, q$ **do**
11 | $i \leftarrow k$-th element of R^A; $j \leftarrow k$-th element of R^B;
12 | $p_i \leftarrow j$;
13 **end**
14 **return** p;

Algorithm 2: Greedy randomized construction procedure

Given two proteins A and B, the construction procedure takes as input their contact maps $C^A = (V_A, E_A)$ and $C^B = (V_B, E_B)$ of lengths n and m ($m > n$),

respectively, and outputs a vector p of length n, where $p_i = \texttt{nil}$ if residue $i \in V_A$ is not aligned, and $p_i = j$ if residue $i \in V_A$ is aligned with residue $j \in V_B$.

In line 1 of Algorithm 2, the number q of residues to be aligned is randomly selected with uniform probability from the interval $[\lceil \alpha \times n \rceil, n]$, where $\alpha \in (0, 1]$ is a positive real valued input parameter. Let $R^A \subseteq V_A$ and $R^B \subseteq V_B$ be the sets of residues from proteins A and B, respectively, that will be aligned. They are initialized empty in line 2. In the **for** loop in lines 3 to 8, q residues are randomly selected from V_A and V_B, greedily favoring nodes with high degree. High degree nodes have a greater chance of being endpoints of isomorphic edges than do low degree nodes. These residues are added, respectively, to sets R^A and R^B. In line 9, the elements of sets R^A and R^B are sorted in increasing order. Finally, in the **for** loop in lines 10 to 14 the k-th residue of R^A is aligned with the k-th element of R^B, for $k = 1, \ldots, q$.

4.2 Approximate local search

Since there is no guarantee that the construction procedure presented in Section 4.1 produces a local maximum number of overlaps, a local improvement procedure can be applied starting at the constructed solution p to attempt to increase the number of overlaps. Given a starting solution p, a local improvement strategy examines solutions in the neighborhood $\mathcal{N}(p)$ of p and replaces p by some solution $p' \in \mathcal{N}(p)$ with $\Lambda(p') > \Lambda(p)$.

Given a solution p, Figure 5 shows four quadrilateral structures that can potentially occur in the solution. In the figures, nodes $r_A^L, r_A^R \in S_A \subseteq V_A$ and $r_B^L, r_B^R \in S_B \subseteq V_B$, while $r_A \in V_A \setminus S_A$ and $r_B \in V_B \setminus S_B$. Each structure has two edges, (r_A^L, r_B^L) and (r_A^R, r_B^R) defined by the bijection f of $\mathcal{L}(S_A, S_B, f)$.

We now describe the neighborhoods of each of the four quadrilateral structures.

- **Type I:** Each quadrilateral structure of Type I in a solution admits two neighbors shown in Figure 6. The first neighbor is obtained by removing edge (r_A^L, r_B^L). This move corresponds to setting $p_i = \texttt{nil}$, where $i = r_A^L$. Likewise, the second neighbor is obtained by removing edge (r_A^R, r_B^R). This move corresponds to setting $p_i = \texttt{nil}$, where $i = r_A^R$. with respect to its contact map, there are $O(n)$ quadrilateral structures of this type.

- **Type II:** Each quadrilateral structure of Type II in a solution admits two neighbors shown in Figure 7. The first neighbor is obtained by replacing edge (r_A^L, r_B^L) by (r_A, r_B^L), where $r_A^L < r_A < r_A^R$. This move corresponds to setting $p_i = \texttt{nil}$ for $i = r_A^L$ and $p_i = j$, where $i = r_A$ and $j = r_B^L$. Likewise, the second neighbor is obtained by replacing edge (r_A^R, r_B^R) by (r_A, r_B^R), where $r_A^L < r_A < r_A^R$. This move corresponds to setting $p_i = \texttt{nil}$ for $i = r_A^R$ and $p_i = j$, where $i = r_A$ and $j = r_B^R$. In the worst case, there are $O(n)$ quadrilateral structures of this type.

- **Type III:** Each quadrilateral structure of Type III in a solution admits two neighbors shown in Figure 8. The first neighbor is obtained by replacing edge (r_A^L, r_B^L) by (r_A^L, r_B), where $r_B^L < r_B < r_B^R$. This move corresponds to setting $p_i = j$, where $i = r_A^L$ and $j = r_B$. Likewise, the second neighbor

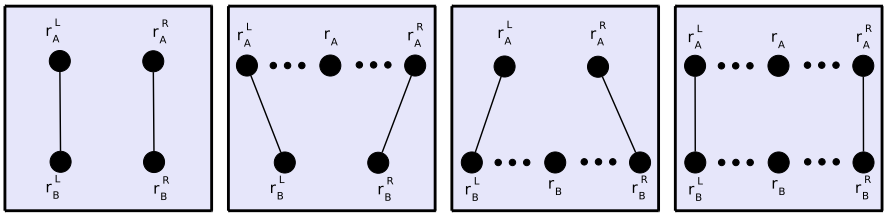

(a) Type A (b) Type B (c) Type C (d) Type D

FIGURE 5 Quadrilateral structures of solution.

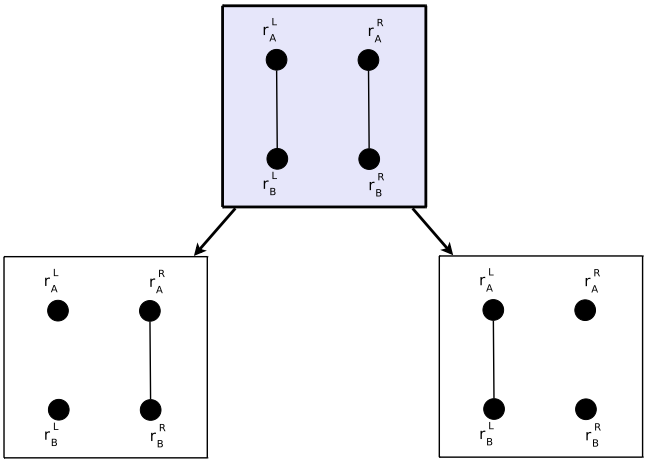

FIGURE 6 Type I moves in local search.

is obtained by replacing edge (r_A^R, r_B^R) by (r_A^R, r_B), where $r_B^L < r_B < r_B^R$. This move corresponds to setting $p_i = j$, where $i = r_A^R$ and $j = r_B$. In the worst case, there are $O(m)$ quadrilateral structures of this type.

- **Type IV:** Each quadrilateral structure of Type IV in a solution admits five neighbors shown in Figure 9. The first neighbor (middle structure in the figure) is obtained by adding edge (r_A, r_B), where $r_A^L < r_A < r_A^R$ and $r_B^L < r_B < r_B^R$. This move corresponds to setting $p_i = j$, where $i = r_A$ and $j = r_B$. The second neighbor (top left structure in the figure) is obtained by replacing edge (r_A^L, r_B^L) by (r_A^L, r_B), where $r_B^L < r_B < r_B^R$. This move corresponds to setting $p_i = j$, where $i = r_A^L$ and $j = r_B$. The third neighbor (top right structure in the figure) is obtained by replacing edge (r_A^R, r_B^R) by (r_A^R, r_B), where $r_B^L < r_B < r_B^R$. This move corresponds to setting $p_i = j$, where $i = r_A^R$ and $j = r_B$. The fourth neighbor (bottom left structure in the figure) is obtained by replacing edge (r_A^L, r_B^L) by (r_A, r_B^L), where

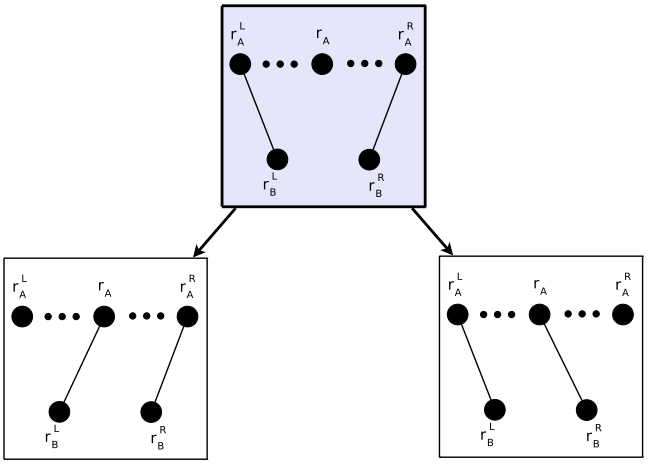

FIGURE 7 Type II moves in local search.

$r_A^L < r_A < r_A^R$. This move corresponds to setting $p_i = \texttt{nil}$ for $i = r_A^L$ and $p_i = j$, where $i = r_A$ and $j = r_B^L$. Finally, the fifth neighbor (bottom right structure in the figure) is obtained by replacing edge (r_A^R, r_B^R) by (r_A, r_B^R), where $r_A^L < r_A < r_A^R$. This move corresponds to setting $p_i = \texttt{nil}$ for $i = r_A^R$ and $p_i = j$, where $i = r_A$ and $j = r_B^R$. In the worst case, there are $O(mn)$ quadrilateral structures of this type.

In a standard local search, one explores the neighborhood of a solution and moves either to the first or to the best improving solution. In either situation, in the worst case, the entire neighborhood will need to be explored at least once. Such large neighborhoods are expensive to explore with a standard local search method. To avoid exploring the entire neightborhood, we propose an approximate local search scheme similar to the one introduced in (Mateus et al., 2009).

The idea of the approximate local search is to sample the neighborhood of the current solution at most $MaxItr$ times or until $MaxCLS$ improving neighbors

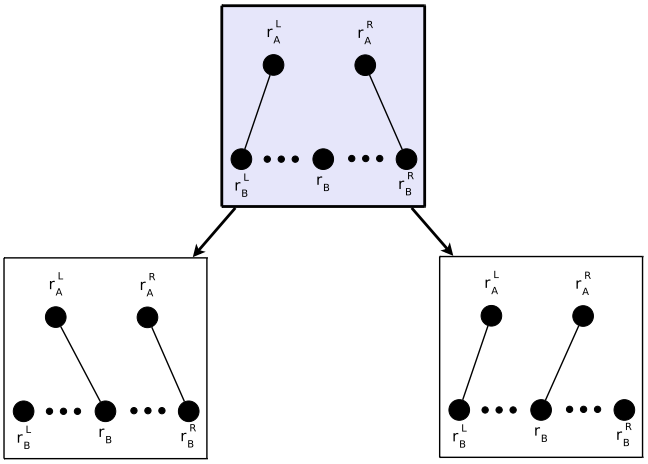

FIGURE 8 Type III moves in local search.

are identified. The search then moves from the current solution p to an improving sampled neighbor p' that is randomly chosen with probability proportional to $\Lambda(p')$. The search repeats until no improved neighbors are found after $MaxItr$ probes. Algorithm 3 shows pseudocode for the approximate local search procedure. The procedure takes as input: the starting solution p, the maximum size $MaxCLS$ of the candidate local search set CLS, the maximum number $MaxItr$ of times the neighborhood of the current solution is sampled, and a parameter k that determines the maximum number of consecutive moves from the current solution p. The loop in lines 1 to 28 is repeated until no improving sampled solution is found, i.e. $CLS = \emptyset$. In line 2, the sampled solution counter $count$ and set $MaxCLS$ are initialized. The loop in lines 3 to 24 is repeated until either the set CLS is full or $MaxItr$ neighbors of p are sampled. In line 4 the current solution is saved as p'.

Starting from p, the **for** loop in lines 5 to 19 performs a number of moves. This number of moves is chosen uniformly at random in the range $[1, \ldots, k]$. Recall

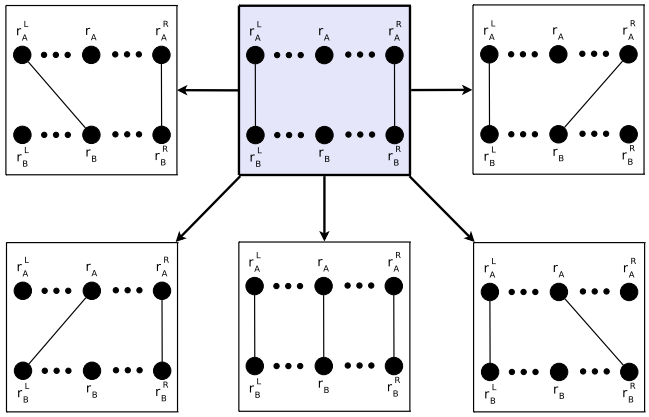

FIGURE 9 Type IV moves in local search.

that a quadrilateral structure is made up of four related nodes, $r_A^L, r_A^R \in S_A$ and $r_B^L, r_B^R \in S_B$, such that r_A^L and r_A^R are, respectively, aligned with r_B^L and r_B^R, and no other alignment exists between these two edges. Therefore, given one of the four nodes, the other three are entirely determined. We call this seed node an *anchor*. In line 6, position of the anchor is chosen at random to be one of the following: left-C^A, right-C^A, left-C^B, or right-C^B. Once the archor position is fixed, line 7 determines the set $\mathcal{R}$ of residues for the anchor. Let Γ_A and Γ_B be the set of aligned residues in C^A and C_B, respectively. Let $i_L^A = \inf \Gamma_A$ and $i_R^A = \sup \Gamma_A$ be, respectively, the leftmost and the rightmost aligned residue of C^A. Similarly, let $i_L^B = \inf \Gamma_B$ and $i_R^B = \sup \Gamma_B$ be, respectively, the leftmost and the rightmost aligned residue of C^B. If the anchor position is

- left-C^A, then $\mathcal{R} = \Gamma_A \setminus \{i_R^A\}$,
- right-C^A, then $\mathcal{R} = \Gamma_A \setminus \{i_L^A\}$,
- left-C^B, then $\mathcal{R} = \Gamma_B \setminus \{i_R^B\}$,

- right-C^B, then $\mathcal{R} = \Gamma_B \setminus \{i_L^B\}$.

Let $\deg(r)$ be the degree of $r \in \mathcal{R}$ with respect to its contact map. In line 8, the anchor residue r is selected at random from $\mathcal{R}$ with probability proportional to $\deg(r)$. In line 9, the quadrilateral structure $\mathcal{Q} = \{r_A^L, r_A^R, r_B^L, r_B^R\}$ is determined. If the anchor position is

- left-C^A, then $r_A^L = r$, r_A^R is the first aligned residual to the right of r_A^L, r_B^L and r_B^R are the residues aligned, respectively, with r_A^L and r_A^R;
- right-C^A, then $r_A^R = r$, r_A^L is the first aligned residual to the left of r_A^R, r_B^L and r_B^R are the residues aligned, respectively, with r_A^L and r_A^R;
- left-C^B, then $r_B^L = r$, r_B^R is the first aligned residual to the right of r_B^L, r_A^L and r_A^R are the residues aligned, respectively, with r_B^L and r_B^R;
- right-C^B, then $r_B^R = r$, r_B^L is the first aligned residual to the left of r_B^R, r_A^L and r_A^R are the residues aligned, respectively, with r_B^L and r_B^R.

Depending on which type of quadrilateral structure $\mathcal{Q}$ is, the appropriate move updates solution p' in lines 10 to 18. In lines 20 to 22, if p' is better than the current solution p, it is added to the set CLS. In line 23, the sampled solution counter $count$ is incremented. After completing the **repeat** loop in lines 3 to 24, if the set CLS is not empty, then in line 26, the new current solution p is randomly selected from set CLS with probability proportional to $\Lambda(p)$.

Procedures `MoveTypeI`, `MoveTypeII`, `MoveTypeIII`, and `MoveTypeIV` are described next. Each procedure takes as input a solution p and a compatible quadrilateral structure $\mathcal{Q}$ and output a solution in the its neighborhood.

```
procedure ApproximateLocalSearch
   Input: p, MaxCLS, MaxItr, k
   Output: Approximate local maximum p
1  repeat
2      count ← 0; CLS ← ∅;
3      repeat
4          p′ ← p;
5          for i = 1, ..., UNIF{1, 2, ..., k} do
6              Randomly select anchor position;
7              Determine allowable set R of residues for anchor;
8              Select anchor residue r ∈ R with prob(r) ∼ deg(r);
9              Determine Q = {r_A^L, r_A^R, r_B^L, r_B^R};
10             case Q is of Type I
11                 p′ ← MoveTypeI(p′);
12             case Q is of Type II
13                 p′ ← MoveTypeII(p′);
14             case Q is of Type III
15                 p′ ← MoveTypeIII(p′);
16             otherwise
17                 p′ ← MoveTypeIV(p′);
18             end
19         end
20         if Λ(p′) > Λ(p) then
21             CLS ← CLS ∪ {p′};
22         end
23         count ← count + 1;
24     until |CLS| ≥ MaxCLS or count ≥ MaxItr ;
25     if CLS ≠ ∅ then
26         Randomly select a solution p ∈ CLS;
27     end
28 until CLS = ∅ ;
29 return p;
```

Algorithm 3: Pseudo-code for `ApproxLocalSearch`: Approximate local search procedure.

Pseudocode for procedure `MoveTypeI` is shown in Algorithm 4. This procedure simply moves to one of the two Type I neighbors of p with equal probability. In line 1, a coin toss is simulated to select the edge to be removed from p. If the outcome of the coin toss is heads, then in lines 3 and 7, edge (r_A^L, r_B^L) is removed. Otherwise, in lines 5 and 7, edge (r_A^R, r_B^R) is removed.

Pseudocode for procedure `MoveTypeII` is shown in Algorithm 5. This procedure moves to one of the two Type II neighbors of p with equal probability. In line 1, a residue r_A located between r_A^L and r_A^R is randomly selected with proba-

bility proportional to $\deg(r_A)$. In line 2, a coin toss is simulated to select the edge to be removed from p. If the outcome of the coin toss is heads, then in lines 4 and 8 edge (r_A^L, r_B^L) is replaced by edge (r_A, r_B^L). Otherwise, in lines 6 and 8, edge (r_A^R, r_B^R) is replaced by edge (r_A, r_B^R).

procedure `MoveTypeI`
  Input: r_A^L, r_A^R, r_B^L, r_B^R, p
  Output: Assignment vector p
1 Randomly select $\pi \in \text{UNIF}(0, 1)$;
2 **if** $\pi < 0.5$ **then**
3 | $i \leftarrow r_A^L$;
4 **else**
5 | $i \leftarrow r_A^R$;
6 **end**
7 $p_i \leftarrow$ `nil`;
8 **return** p;

Algorithm 4: Type I move in approximate local search

procedure `MoveTypeII`
  Input: r_A^L, r_A^R, r_B^L, r_B^R, p
  Output: Assignment vector p
1 Randomly select r_A, $r_A^L < r_A < r_A^R$, with $\text{prob}(r_A) \sim \deg(r_A)$;
2 Randomly select $\pi \in \text{UNIF}(0, 1)$;
3 **if** $\pi < 0.5$ **then**
4 | $j \leftarrow r_B^L$;
5 **else**
6 | $j \leftarrow r_B^R$;
7 **end**
8 $i \leftarrow r_A$; $p_i \leftarrow j$;
9 **return** p;

Algorithm 5: Type II move in approximate local search

Pseudocode for procedure `MoveTypeIII` is shown in Algorithm 6. This procedure moves to one of the two Type III neighbors of p with equal probability. In line 1, a residue r_B located between r_B^L and r_B^R is randomly selected with probability proportional to $\deg(r_B)$. In line 2, a coin toss is simulated to select the edge to be removed from p. If the outcome of the coin toss is heads, then in lines 4 and 8 edge (r_A^L, r_B^L) is replaced by edge (r_A^L, r_B). Otherwise, in lines 6 and 8, edge (r_A^R, r_B^R) is replaced by edge (r_A^R, r_B).

```
procedure MoveTypeIII
   Input: r_A^L, r_A^R, r_B^L, r_B^R, p
   Output: Assignment vector p
1  Randomly select r_B such that r_B^L < r_B < r_B^R;
2  Randomly select π ∈ UNIF(0, 1);
3  if π < 0.5 then
4  |  i ← r_A^L;
5  else
6  |  i ← r_A^R;
7  end
8  j ← r_B; p_i ← j;
9  return p;
```

Algorithm 6: Type III move in approximate local search

Pseudocode for procedure `MoveTypeIV` is shown in Algorithm 7. This procedure moves to one of the five Type IV neighbors of p. In line 1, residue r_A, located between r_A^L and r_A^R is randomly selected with probability proportional to $\deg(r_A)$. Likewise, in line 2, residue r_B, located between r_B^L and r_B^R is randomly selected with probability proportional to $\deg(r_B)$. In line 3, a coin toss is simulated to determine whether a new edge will be added or if one will be replaced. If the outcome of the coin toss is heads, then in lines 18 and 20 edge (r_A, r_B) is added. Otherwise two simultaneous coin tosses are simulated to determine which

of the other four neighborhood solutions will be selected for the move. If is the outcome is two heads, then in lines 7 and 20, edge (r_A^L, r_B^L) is replaced by edge edge (r_A^L, r_B). If is the outcome of the first coin is heads and of the second tails, then in lines 9 and 20, edge (r_A^R, r_B^R) is replaced by edge edge (r_A^R, r_B). If is the outcome of the first coin is tails and of the second heads, then in lines 11, 12, and 20, edge (r_A^R, r_B^R) is replaced by edge edge (r_A, r_B^R). Finally, if is the outcome is two tails, then in lines 14, 15, and 20, edge (r_A^L, r_B^L) is replaced by edge edge (r_A, r_B^L).

4.3 Path-relinking

Path-relinking (Glover, 1996) is an intensification scheme that explores paths in the solution space connecting two good-quality (or elite) solutions. Given two solutions of the MAX-CMO problem denoted by their respective assignment vectors s and t, let $\Delta(s,t) = \{i = 1,\ldots,n : \ s_i \neq t_i\}$. Path-relinking examines each solution in the path $s = p_1(s,t), p_2(s,t), \ldots, p_k(s,t) = t$ connecting s and t, where $k = |\Delta(s,t)|$ and $p_j(s,t)$ is the j-th solution in the path from s to t. Solution $p_j(s,t) \in \mathcal{N}(p_{j-1}(s,t))$ such that $|\Delta(p_j(s,t),t)| = |\Delta(p_{j-1}(s,t),t)| - 1$, i.e. $p_j(s,t)$ is obtained by reassigning a residue $\ell \in \Delta(p_{j-1}(s,t),t)$ of $p_{j-1}(s,t)$ to t_ℓ. It is easy to verify that for any pair of solutions s and t there will be at least one path of the type described above from s to t.

Algorithm 8 illustrates the pseudo-code of the path-relinking procedure applied to a pair of solutions s (starting solution) and t (target solution).

The procedure starts in line 1 by computing set $\Delta(s,t) = \{i = 1,\ldots,n : s_i \neq t_i\}$ comprised of the set of indices for which the residues in s and t differ. In

procedure `MoveTypeIV`
Input: $r_A^L, r_A^R, r_B^L, r_B^R, p$
Output: Assignment vector p
Randomly select r_A such that $r_A^L < r_A < r_A^R$;
Randomly select r_B such that $r_B^L < r_B < r_B^R$;
Randomly select $\pi_1 \in \mathrm{UNIF}(0, 1)$;
if $\pi_1 < 0.5$ **then**
  Randomly select $\pi_2 \in \mathrm{UNIF}(0, 1)$;
  case $\pi_2 \leq 0.25$
    $i \leftarrow r_A^L$; $j \leftarrow r_B$;
  case $0.25 < \pi_2 \leq 0.5$
    $i \leftarrow r_A^R$; $j \leftarrow r_B$;
  case $0.5 < \pi_2 \leq 0.75$
    $i \leftarrow r_A^R$; $p_i \leftarrow$ `nil`;
    $i \leftarrow r_A$; $j \leftarrow r_B^R$;
  otherwise
    $i \leftarrow r_A^L$; $p_i \leftarrow$ `nil`;
    $i \leftarrow r_A$; $j \leftarrow r_B^L$;
  end
else
  $i \leftarrow r_A$; $j \leftarrow r_B$;
end
$p_i \leftarrow j$;
return p;

Algorithm 7: Type IV move in approximate local search

```
procedure PathRelinking
   Input: Pair of solutions s and t
   Output: Best solution x* in path from s to t
1  Compute set Δ(s,t) ← {i = 1,...,n : s_i ≠ t_i};
2  x* ← argmax{Λ(s), Λ(t)};
3  Λ* ← Λ(x*);
4  x ← s;
5  while Δ(x,t) ≠ ∅ do
6      Define Δ'(x,t) ⊆ Δ(x,t) to be the set of feasible residues;
7      i* ← argmax{Λ(x ⊕ i) : i ∈ Δ'(x,t)};
8      Δ(x ⊕ i*,t) ← Δ(x,t) \ {i*};
9      x ← x ⊕ i*;
10     if not ISFeasible(x) then
11         Repair(x,i);
12     end
13     if Λ(x) > Λ* then
14         Λ* ← Λ(x);
15         x* ← x;
16     end
17 end
18 return x*;
```

Algorithm 8: Path-relinking between solutions s and t.

lines 2 and 3, the best solution x^* among s and t and its cost Λ^* are determined. In line 4 the current solution x is initialized to s. The loop in lines 5 to 17 is repeated until the path is traversed, i.e. the current solution s is a neighbor of the target t. In line 6, the set of feasible indices $\Delta'(x,t)$ is defined to be the set of indices $i \in \Delta(x,t)$ for which the assignment $y = (x_1, \ldots, x_{i-1}, t_i, x_{i+1}, \ldots, x_n)$ is feasible. We use the shorthand notation $y = x \oplus i$ to represent this move. If the constraints of this new solution are not violated, the new solution is feasible. Otherwise, a repair procedure is applied in an attempt to make it feasible in lines 10 to 12. The repair procedure simply removes all alignments that are vialating any of the constraints, maintaining the alignment i of the solution target.

In line 7, the feasible index i^* that results in the highest valued assignment is determined and in line 8 set $\Delta(x \oplus i^*, t)$ is defined to be $\Delta(x,t) \setminus \{i^*\}$. In line 14 the move is made and in lines 13 to 16 the best solution in the path and its value are updated if necessary. The best solution x^* found in the path from s to t is returned in line 18.

5 COMPUTATIONAL EXPERIMENTS AND RESULTS

In this section, we report on computational experiments carried out with the GRASP-PR heuristic introduced in this paper in order to analyze its effectiveness and to compare our algorithm with existing ones. First, we describe our test environment and use datasets, next we analyze and compare our implementation with other heuristics from the literature on a suite of test problems.

5.1 Test environment and Datasets

All experiments with the GRASP-PR were carried out on a Dell PE1950 computer with dual quad core 2.66 GHz Intel Xeon processors and 2 Gb of memory, running Red Hat Linux nesh version 5.1.19.6 (CentOS release 5.2, kernel 2.6.18-53.1.21.el5). The GRASP-PR heuristic was implemented in Java and compiled into bytecode with javac version 1.6.0 05. The random-number generator is a implementation of the Mersenne Twister algorithm (Matsumoto & Nishimura, 1998) from the COLT[‡] library.

TABLE 1 Dataset information. $Pairs$ stand for the number of pairwise comparisons performed. The values for $Avg.Contacts$ corresponds to contact maps at 7Å.

Dataset	Pairs	Avg. Residues	Avg. Contacts	Reference
Lancia	2702	57.07	95.91	(Caprara & Lancia, 2002)
Skolnick	161	158.23	470.93	(Caprara & Lancia, 2002)
Chew-Kedem	145	201.91	928.75	(Chew & Kedem, 2002)

For the test bed analysis, we used three datasets[§] (see table 1): The Lancia dataset (Caprara & Lancia, 2002) with 269 proteins and 2702 different instances of protein pairs, the Skolnick datset (Caprara & Lancia, 2002) with 40 proteins and

[‡]COLT is a open source library for high performance scientific and technical computing in Java. See *http://acs.lbl.gov/∼hoschek/colt/*

[§]The datasets can be downloaded at `http://goic.dcc.ufla.br/Biocomp/Datasets.html`

161 different instances of protein pairs, the Chew-Kedem dataset (Chew & Kedem, 2002) with 40 proteins and 145 different instances.

5.2 Comparison of the GRASP-PR heuristic with other algorithms

In the first experiment, we use of all instances of the three datasets, totalizing 3008 instances of protein pairs.

Caprara & Lancia (2002) proposed a Lagrangian Relaxation (LR) approach for solving MAX-CMO, where the optimal Lagrange multipliers are found by subgradient optimization. Besides yielding an upper bound on the optimal solution of the original problem, the Lagrangian multipliers are used to drive a heuristic to construct the MAX-CMO solutions. Krasnogor et al. (2003) have demonstrated that this LR algorithm was able to find better results than the previous algorithms for the MAX-CMO over the Chew-Kedem dataset, and after that, the LR was reviewed over different datasets (Caprara et al., 2004; Xie & Sahinidis, 2007) confirming its effectiveness.

Pelta et al. (2008) argued that in order to compare a set of algorithms properly, all of them should be ideally compiled and run in the same computational environment. Hence, the experiments carried out in this study met such a requirement. We make use of the source codes of LR [¶] and VNS[‖] algorithms to perform the comparison.

The VNS heuristic is presented as "a simple and fast" heuristic for protein structure comparison and its original stopping criterion for each run is 100 iterations or 20 iterations without improvements (whatever comes first). Three versions of VNS heuristic are available: MSVNS1, MSVNS2 and MSVNS3. In all computational experiments in this paper, we set the best VNS version and parameter

[¶]The LR algorithm was implemented in C programming language and it was that was kindly provided to us by one of the authors of Caprara & Lancia (2002), Alberto Caprara.

[‖]The VNS algorithm was fully implemented in C++ programming language and the software is available for download at *http://modo.ugr.es/jrgonzalez/msvns4maxcmo*.

looking at the paper: “The best alternative is MSVNS3 with windows sizes of 10-30-50 leading to an average error below 3.6% for Lancia’s dataset with 2702 pairs, and below 1.7% for the Skolnick’s one.” (Pelta et al., 2008).

There are also three different modes of the LR algorithm, which differ by the heuristic used to build the MAX-CMO solutions from the lagrange multipliers. We applied one denoted by LAGR-R which uses local search at the root node only to accomplish it, because according to Xie & Sahinidis (2007) they “recorded the best solutions and CPU time for LAGR-R”.

We also adjusted the best combination of parameters for the GRASP-PR heuristic. To accomplish it, we tested 268 combinations of parameters on 4 randomly selected instances (2 from Lancia, 1 from Chew-Kedem and 1 from Skolnick). We performed 10 runs per parameter combination on each one of the 4 instances, with a running time limit of 1 second and a calculation of the average error of each round. For the four analyzed instances, the parameters that showed a lower average error are: α(delimiter of greedy randomized construction): 0.7, $MaxCLS$ (Local Search parameter) : 20, $MaxItr$ (Local Search parameter) : 10, Local Search moves : 2, $|P|$ (elite set P size) : 8, δ (sufficiently different level) : 2.

After selecting the best versions and parameters for each algorithm, we performed 30 runs on each instance of the selected datasets using MSVNS3 with windows size of 30. For each instance, the minimum, the average and the maximum overlap values of the 30 runs were calculated, as well as the minimum and maximum running times. The average running time of the runs subset that reached the maximum overlap value is also calculated. This last measure of time was set as the stopping criterion for the LR and GRASP-PR algorithms, and then we carried out 30 runs on each instance using these two others algorithms and the minimum, average and maximum overlap values of the 30 runs of these ones

are also calculated. As result of this experiment, complementary data containing the values for each instance of the three datasets is available for download at `http://goic.dcc.ufla.br/Biocomp/ResultsCMOP.xls` as a as a benchmark for MAX-CMO algorithms comparison.

For instances of Lancia and Skolnick datasets, the error per instance of each algorithm was calculated using overlap values** given by the exact algorithm from the algorithm presented in (Xie & Sahinidis, 2004). For instances of Chew-Kedem dataset, for which the exact overlap values were not available, the error(%) was calculated using the Upper Bound values returned by the LR algorithm. In both cases, the error is calculated with respect to the maximum overlap value of the 30 runs per instance. The results are summarized in Tables 1 and 2.

In the experiment conducted by us, the results for the VNS algorithm showed in Table 1 closely corroborate with results presented by Pelta et al. (2008). They report an average error of 3.6% for Lancia dataset and below 1.7% for the Skolnick's. We obtained 3.398% and 1.708%, respectively.

For Lancia dataset, Table 2 shows that the VNS heuristic presents the lowest average error (3.398%) and and the highest number of optimally solved instances (1578 - 58.4%). The LR algorithm obtained the second lowest average error (8.438%) although it has optimally solved fewer instances than the GRASP-PR (970 and 1114 number of optimally solved instances for the LR algorithm and GRASP-PR, respectively). Considering only the instances not optimally solved (Near-Optimally Solved), the average errors increase to 8.160%, 15.512% and 13.150% for VNS, LR and GRASP-PR, respectively. If we rank the algorithms considering the value of average error, for Lancia dataset, we observe that the VNS

**These optimal overlap values were kindly provided by one of the authors of reference Pelta et al., (2008), Juan González, who make use of same values for computing the error of the VNS algorithm in respect to the optimal overlap values.

algorithm is the best one, followed by LR and finally the GRASP-PR. Considering the number of instances optimally solved, the VNS algorithm, the GRASP-PR and the LR, we found out that the Lancia dataset has protein pairs with a smaller number of residues and contacts, containing also the easiest number of instances, despite it having the largest number of them (see table 1).

For the Skolnick dataset, considering the average error of all instances, we rank the algorithms with the VNS (1.708%) as the best heuristic followed by GRASP-PR (3.821%). And considering the number of optimally solved instances, we rank the GRASP-PR - 89 (55.28%) optimally solved instances - as the best one followed by VNS - 63 (39.13%) optimally solved instances. The results for this dataset show that the results of GRASP-PR are competitive with the other two heuristics analyzed.

Table 3 shows results for the Chew-Kedem dataset, where the error is calculated based on the best Upper Bound algorithm value obtained from the LR algorithm. In this table, the results are grouped according to the protein families in order to investigate whether any specific type of structural folding is favoring some enhancement that could further improve the proposed heuristic, which could be attained through analyses and proposition of specialized constructive methods, designed for different families of proteins. Additional result analyses in different protein faimilies of this datasets will be performed. In general, the GRASP-PR algorithm showed the best results, with an average error of 12.412%, followed closely by the LR (12.839%). These results encourage the use of the proposed GRASP-PR heuristic, for the Chew-Kedem is considered the most challenging dataset according to to Krasnogor et al. (2003).

TABLE 2 Results over 2702 pairs from Lancia's dataset, and 161 pair from Skolnick's dataset. The error is measured with respect to the optimum value.

			Error (%)			Time (seconds)					
	Algorithm	**N**	**Avg.**	**SD**	**Median**	**Min.**	**Max.**	**Avg.**	**SD**	**Median**	
Total	VNS	2702 (100%)	3.398	4.882	0.000	0.010	5.189	0.077	0.113	0.062	Lancia's Dataset
	GRASP-PR	2702 (100%)	9.115	13.326	2.679	0.010	5.189	0.077	0.113	0.062	
	LAGR	2702 (100%)	8.438	10.001	4.167	0.010	5.189	0.077	0.113	0.062	
Optimally Solved	VNS	1578 (58.4%)	0.000	0.000	0.000	0.015	0.893	0.083	0.054	0.068	
	GRASP-PR	1114 (41.30%)	0.000	0.000	0.000	0.011	0.608	0.077	0.049	0.065	
	LAGR	970 (35.9%)	0.000	0.000	0.000	0.010	0.893	0.085	0.057	0.070	
Near-Optimally Solved	VNS	1124 (41.6%)	8.160	4.285	8.000	0.010	5.189	0.069	0.162	0.054	
	GRASP-PR	1586 (58.70%)	15.512	14.247	8.554	0.010	5.189	0.077	0.141	0.060	
	LAGR	1732 (64.1%)	13.150	9.691	11.111	0.010	5.189	0.075	0.140	0.059	
Total	VNS	161 (100%)	1.708	2.257	0.606	2.784	47.780	14.046	11.888	6.605	Skolnick's Dataset
	GRASP-PR	161 (100%)	3.821	7.935	0.000	2.784	47.780	14.046	11.888	6.605	
	LAGR	161 (100%)	4.690	5.930	2.493	2.784	47.780	14.046	11.888	6.605	
Optimally Solved	VNS	63 (39.13%)	0.000	0.000	0.000	2.784	33.360	8.782	8.891	4.604	
	GRASP-PR	89 (55.28%)	0.000	0.000	0.000	2.784	35.570	6.060	10.041	6.060	
	LAGR	55 (34.16%)	0.000	0.000	0.000	2.784	47.780	11.203	11.370	5.945	
Near-Optimally Solved	VNS	98 (60.87%)	2.806	2.300	2.116	3.889	47.780	17.430	12.370	9.758	
	GRASP-PR	73(44.72%)	8.544	10.048	5.620	3.495	47.780	18.162	12.745	12.230	
	LAGR	106 (65.84%)	7.124	6.007	5.900	3.243	42.620	15.521	11.935	7.780	

TABLE 3 Results over 145 pairs from Chew-Kedem dataset. The error is measured based on the Upper Bound value given by the Lagrangian Relaxation algorithm.

			Error (%)			Time (seconds)				
	Algorithm	**N**	**Avg.**	**SD**	**Median**	**Min.**	**Max.**	**Avg.**	**SD**	**Median**
All Pairs	VNS	145 (100%)	12.839	11.104	9.626	2.033	75.290	10.728	12.839	7.422
	GRASP-PR	145 (100%)	12.412	12.850	6.497	2.033	75.290	10.728	12.839	7.422
	LAGR	145 (100%)	9.756	11.885	5.398	2.033	75.290	10.728	12.839	7.422
Globin Pairs	VNS	102 (70.34%)	9.039	3.348	8.867	5.452	17.990	7.840	2.097	7.416
	GRASP-PR	102 (70.34%)	6.648	3.416	8.867	5.452	17.990	7.840	2.097	7.416
	LAGR	102 (70.34%)	5.209	2.090	4.881	5.452	17.990	7.840	2.097	7.416
Alpha-Beta Pairs	VNS	13 (8.97%)	16.918	21.046	2.667	10.120	30.540	18.262	9.014	12.270
	GRASP-PR	13 (8.97%)	17.612	22.121	2.000	10.120	30.540	18.262	9.014	12.270
	LAGR	13 (8.97%)	18.074	22.763	2.000	10.120	30.540	18.262	9.014	12.270
Beta Pairs	VNS	15 (10.34%)	14.320	4.890	14.079	3.350	5.173	4.139	0.551	4.037
	GRASP-PR	15 (10.34%)	27.355	9.707	29.130	3.350	5.173	4.139	0.551	4.037
	LAGR	15 (10.34%)	11.500	5.030	11.905	3.350	5.173	4.139	0.551	4.037
TIM-Barrel Pairs	VNS	6 (4.14%)	35.474	11.756	39.383	61.080	75.290	67.832	5.970	67.255
	GRASP-PR	6 (4.14%)	32.766	5.720	34.374	61.080	75.290	67.832	5.970	67.255
	LAGR	6 (4.14%)	31.046	12.518	35.821	61.080	75.290	67.832	5.970	67.255
Mixed Pairs	VNS	9 (4.14%)	32.448	15.905	30.631	2.033	10.280	5.463	3.313	4.976
	GRASP-PR	9 (4.14%)	30.770	17.140	30.040	2.033	10.280	5.463	3.313	4.976
	LAGR	9 (4.14%)	32.175	16.751	30.040	2.033	10.280	5.463	3.313	4.976

5.3 Time-to-target plots for GRASP-PR against other heuristics

n the following experiment, we used of eight randomly selected instances: 4 from dataset Lancia, 2 from Skolnick and 2 from the Chew-Kedem one. Information on these instances is summarized in the table 4.

TABLE 4 Eight randomly selected instances for plotting the time-to-target. In the following, we use their assigned indexes to refer to the respective instances. Column with identifier *ID* refer to the index assigned to instance; columns with identifier *Prot.* refer to the PDB code for the protein; columns with identifiers *Res.* and *Contacts* refer to the number of residues and contacts of their contact maps constructed at 7Å, and column with identifier *Target Value* refers the optimal value for the instance that will be used as target value in analysis of time-to-target.

ID	Prot. 1	Res.	Contacts	Prot. 2	Res.	Contcts	Target Value	Dataset
1	1gzi	58	110	9msi	59	112	106	Lancia
2	1ekl	58	106	1msj	59	114	103	Lancia
3	1eqt	58	101	1hcc	47	75	55	Lancia
4	1fh3	54	86	1ptx	54	93	57	Lancia
5	3chy	128	378	4tmy	118	366	323	Skolnick
6	1pla	97	275	1pcy	99	282	253	Skolnick
7	1babA	142	412	1mba	146	439	347	Chew-Kedem
8	1aa9	171	528	1ct9A	497	1508	280	Chew-Kedem

Time-to-target (TTT) plots display on the ordinate axis the probability that an algorithm will find a solution at least as good as a given target value within a given running time, shown on the abscissa axis. TTT plots were used by Feo et al. (1994) and have been advocated thenceforward as a way to characterize the running times of stochastic algorithms for combinatorial optimization.

In this analysis, each heuristic is run n times on the fixed instance and using the given target solution value. For each of the n runs, the random number generator is initialized with a distinct seed and, therefore, the runs are assumed to be independent. For each instance/target pair, the running times are sorted in increasing order. We associate with the $i-th$ sorted running time t_i a probability

$p_i = (i - 1/2)/n$ and plot the points $z_i = [t_i, p_i], \text{for} i = 1, ..., n.$. Then, this cumulative probability distribution is ploted allowing to infer and compare details and information about the performance of the heuristics.

For each of the selected instances, we made 200 independent runs of the GRASP-PR, 200 runs of the VNS and 200 runs of the LR algorithm. Each of these runs stopped when the target-valued solution (Target Value - Table 4) was found, and we record the time taken for each run. Figure 10 and 11 shows TTT plots for all algorithms analyzed on all instances from Table 4. These plots display the empirical probability distributions of the random variable time to target solution. Each heuristic was run a total of 1600 times in the experiments.

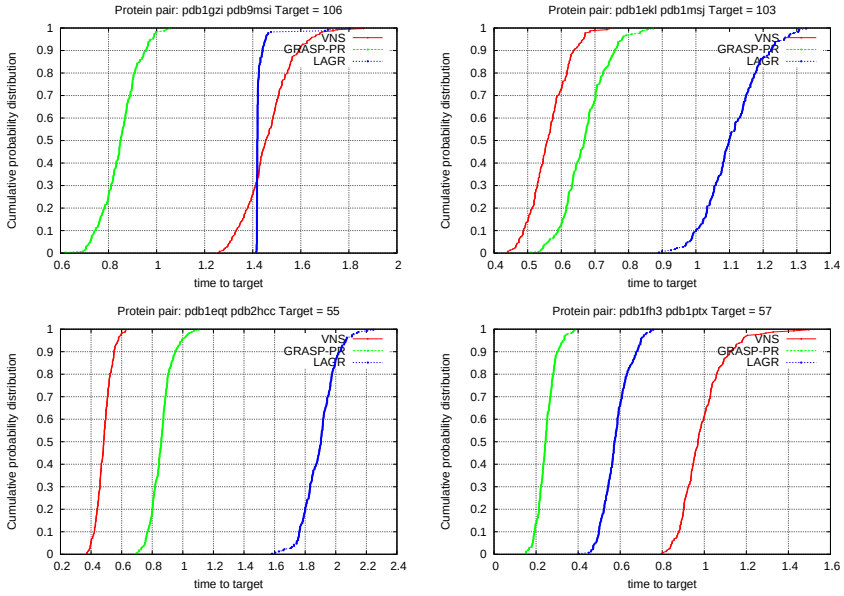

FIGURE 10 Time-to-target plots. Plots of cumulative probability distributions of GRASP-PR, VNS and LR running times for instances 1, 2, 3, and 4 (see table 4).

The relative position of the curves to the feft implies that, given a fixed amount

of computing time, the algorithm refered to that curve has a higher probability than grasp of finding a target solution. The relative position of the curves to the right implies that, given a fixed probability of finding a target solution, the expected time taken by the algorithm refered to that curve to find a solution with that probability is greater than the time taken by the other ones. For example, consider instance 6 in Figure 11. The probability of finding a target at least as good as the target value 253 in 3.5 seconds is approximately of 40% for all algorithms. In 4.0 seconds at the most, these probabilities increase to approximately 90% for GRASP-PR and 85% for VNS and LR.

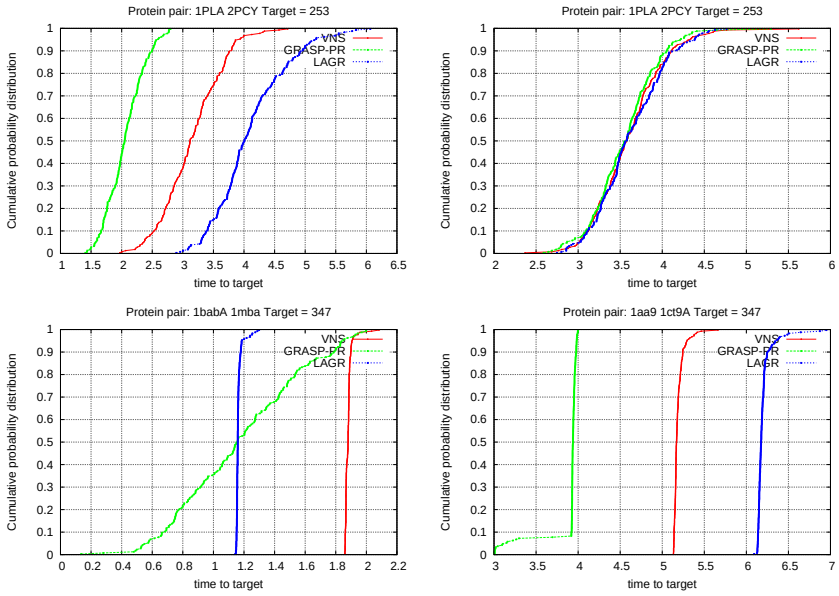

FIGURE 11 Time-to-target plots. Plots of cumulative probability distributions of GRASP-PR, VNS and LR running times for instances 5, 6, 7, and 8 (see table 4).

Figure 10 show that the algorithm VNS has a small dominance over the GRASP-PR in two cases (instances 1 and 4), and the opposite in the other two: for in-

stances 2 and 3 the GRASP-PR demonstrates to be better. These figures are plots over instances of the dataset Lancia with smaller number of residues and contacts, then easier instances, and maybe favoring simple heuristics as the VNS. Figure 11 shows the dominance of GRASP-PR for instances 5 and 8, and for instances 6 and 7 there are two cases where it is not possible to identify a clear dominance. These results demonstrate that the proposed algorithm is very competitive compared the other algorithms analyzed.

5.4 GRASP-PR and the Skolnick Clustering test set

The aim of the Skolnick clustering test originally suggested by Skolnick and described in (Lancia et al., 2001) is to classify 40 proteins into four families according to their cluster membership. The proteins belonging to this dataset are shown in Table 1. In the following, we use their assigned indexes to refer to the respective proteins.

TABLE 5 Protein structures of the Skolnick test set. Columns with identifier ID refer to the index assigned to the proteins; columns with identifier PDB refer to the PDB code for the protein containing the protein; and columns with identifier CID refer to the chain index of a protein. If a protein consists of a single chain, the corresponding entry in the CID column is -. Note that the IDs differ from those used in (Lancia et al., 2001).

ID	**PDB**	**CID**	**ID**	**PDB**	**CID**	**ID**	**PDB**	**CID**	**ID**	**PDB**	**CID**
1	1b00	A	*11*	1rn1	C	*21*	2b3i	A	*31*	1tri	-
2	1dbw	A	*12*	3chy	B	*22*	2pcy	-	*32*	3ypi	A
3	1nat	-	*13*	4tmy	A	*23*	2plt	-	*33*	8tim	A
4	1ntr	-	*14*	4tmy	B	*24*	1amk	-	*34*	1ydv	A
5	1qmp	A	*15*	1baw	A	*25*	1aw2	A	*35*	1b71	A
6	1qmp	B	*16*	1byo	A	*26*	1b9b	A	*36*	1bcf	A
7	1qmp	C	*17*	1byo	B	*27*	1btm	A	*37*	1dps	A
8	1qmp	D	*18*	1kdi	-	*28*	1hti	A	*38*	1fha	-
9	1rn1	A	*19*	1nin	-	*29*	1tmh	A	*39*	1ier	-
10	1rn1	B	*20*	1pla	-	*30*	1tre	A	*40*	1rcd	-

Table 2 describes the proteins and their families. Its fourth column with iden-

tifier *Seq. Sim.* indicates that sequence alignment fails for clustering the protein according to their family membership. This motivates structural alignment for solving the Skolnick clustering test.

TABLE 6 Protein domains of the Skolnick test set and their categories as taken from (Caprara & Lancia, 2002).Shown are the characteristics of the four families, the mean number of residues, the range of similarity obtained by sequence alignment and the identifiers of the proteins.

Family	**Style**	**Residues**	**Seq-Sim.**	**Proteins**
1	alpha-beta	124	15-30%	1-14
2	beta	99	35-90%	15-23
3	alpha-beta	250	30-90%	24-34
4	-	170	7-70%	35-40

The GRASP-PR algorithm and the server's one are applied in an all-against-all fashion to the dataset and a distance matrix is calculated. The GRASP-PR running time limit is adjusted to 0.5 seconds, thereby, for the 780 pairwise structural alignments the process required about 10 minutes. As overlap values are not adequate *per se* for classification purposes because such values depend on the size of the proteins being compared, it is applied a normalization scheme, according to (Pelta et al., 2008), it may play a crucial role in protein classification. There is no general agreement on how to do normalization, so we use two of the available alternatives - first and second alternatives were proposed in (Lancia & Istrail, 2004) and (Xie & Sahinidis, 2004), respectively:

$$Norm1(P_i, P_j) = \frac{overlap(P_i, P_j)}{min(contactsP_i, contactsP_j)} \tag{1}$$

$$Norm2(P_i, P_j) = \frac{2 * overlap(P_i, P_j)}{contactsP_i + contactsP_j} \tag{2}$$

Finally, with the values of the distance matrix normalized by ***Norm1*** and

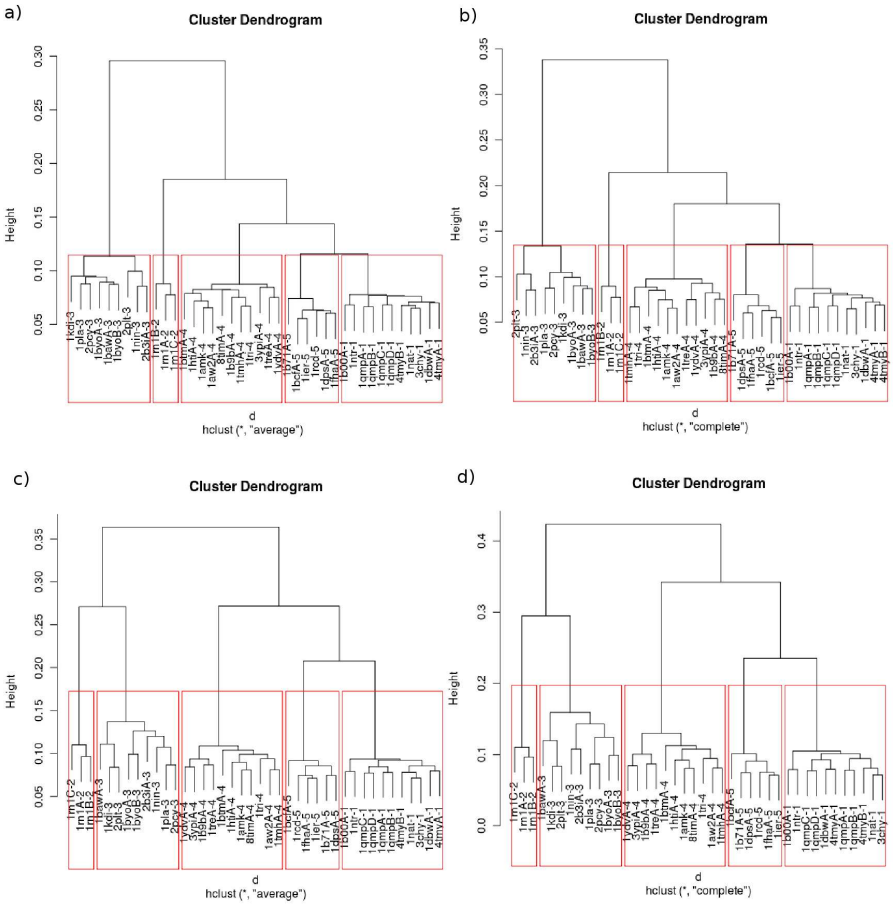

FIGURE 12 Hierarchical Clustering based on the normalized overlap values among proteins in Skolnick's dataset. The upper dendrograms (a, b) correspond to the avarage and complete linkage clustering using ***Norm1*** and the lower ones (c, d) to the avarage and complete linkage clustering using ***Norm2***.

Norm2, we apply complete and average linkage hierarchical clustering as implemented in R software package with the final objective of evaluating if the strategy is able to detect similarity at SCOP's fold level (Murzin et al., 1995). We can see the dendograms generated by Goic-Biocomp server in Figure 1. For visualization purposes, the class number is displayed at the right of the protein name.

The results indicate an agreement with the SCOP categories as shown in Table 3. The GRASP-PR heuristic is able to perfectly recover the original grouping independently of the normalization and clustering algorithms, since it successfully classified the Skolnick proteins into five families according to the SCOP classification levels.

TABLE 7 Descriptions of the proteins clusters from the Skolnick's test. Fold,family, and superfamily are according to SCOP.

Cluster	Proteins	Fold/Superfamily/Family
1	1-8, 12-14	Flavodin-like Che Y-like Che Y-related
2	9-11	Microbial ribonucleases Microbial ribonucleases Fungi ribonucleases
3	15-23	Cuperdoxin-like Cuperdoxins Plastocyanim/Plastoazurin-like
4	24-34	TIM-beta alpha-barrel Triosephosphate isomerase (TIM) Triosephosphate isomerase (TIM)
5	35-40	Ferritin-like Ferritin-like Ferritin

5.5 GRASP-PR as a structural alignment tool

For a protein structure alignment algorithm, it is important to investigate whether it produces biologically meaningful alignments. In this computational experiment we aim to investigate whether our heuristic provides biologically meaningful align-

ments for practical instances, besides to investigate whether GRASP-PR can replicate the results obtained by exact methods but with less computational effort and a simple strategy. To accomplish it, we use the MAX-CMO solution to guide the superimposition of proteins pairs and we make a visual inspection of these ones, as well as we perform analysis of the RMSD value, comparing the results of GRASP-PR against the successful exact algorithm "Exact-Reduction Based (RB) algorithm" proposed by (Xie & Sahinidis, 2007).

To superpose two protein structures one must have a mapping between equivalent amino acids in the two proteins. We can use the MAX-CMO solution as this required mapping which is used to guide the superimpositioning. So, after calculating the mapping between equivalent amino acids of the two proteins via MAX-CMO solution, we make use of a Biopython (Cock et al., 2009) script to create a PDB file with the two structures superposed.

The root mean square deviation (RMSD) is the measure of the average distance between the backbones of superimposed proteins. Unlike the number of overlaps found by MAX-CMO algorithms, the lower the RMSD to superpose the protein pair given the residues mapping, and also to calculate the RMSD value calculated for two superimposed proteins, more similar they are.

In this experiment, we use five instances selected at random from different datasets. The contact maps are constructed with a threshold of 6.5Å - see Table 4. Based on this test set, we compare GRASP-PR against the RB algorithm in terms of overlaps value and RMSD. The running time limit for the GRASP-PR heuristic is set to 5 seconds, while the RB, as a exact algorithm, just stop running as the optimal value is found. Table 5 compare the two algorithms in terms of overlaps value of MAX-CMO solutions and RMSD resultant of the superimposition.

As we can see in table 5, in terms of the overlaps and RMSD values, our

TABLE 8 Test set description. In the following, we use their assigned indexes to refer to the respective protein pair.

Instance	Protein 1	Protein 2	Dataset
1	1ash	1hlm	Chew-Kedem (Chew & Kedem, 2002)
2	1qfo	1neu	Chew-Kedem (Chew & Kedem, 2002)
3	2ach	7api	Leluk-Konieczny-Roterman (Leluk et al., 2003))
4	1rcd	1ier	Skolnick (Caprara & Lancia, 2002)
5	4tmt	1qmpB	Skolnick (Caprara & Lancia, 2002)

TABLE 9 Test results of the five selected proteins pairs. In the table is shown the running time, overlaps value/ the error (%) with respect to the optimal value of MAX-CMO, the RMSD value found by each algorithm over each instance.

	$Time$(s)		$Overlap/Error(\%)$		$RMSD$	
Instance	**GRASP-PR**	**RB**	**GRASP-PR**	**RB**	**GRASP-PR**	**RB**
1	5.00	754.40	271(2.87%)	279(0.00%)	5.21	3.19
2	5.00	185.8	156(13.33%)	180(0.00%)	3.01	2.77
3	5.00	3746.3	700(0.28%)	702(0.00%)	1.31	1.39
4	5.00	48.58	448(0.00%)	448(0.00%)	0.65	0.65
5	5.00	55.25	255(0.00%)	255(0.00%)	1.18	1.18

algorithm is very competitive with the exact algorithm from (Xie & Sahinidis, 2007), since the error with respect to the optimal value is 0.00 for instances 4 and 5, and very low for the other instance 1, 2 and 3 - 2.87%, 13.33% and 0.28%, respectively. For instances 4 and 5, the RMSD value found by GRASP-PR is as lower as the ones found by the RB algorithm, and for instances 1 and 2 this difference is very small. These results are very impressive particularly considering that the running time of GRASP-PR heuristic is about 10x to 750x lower than the running time of the RB algorithm.

For instance 3, we have an interesting particular case: although the overlap value found by the GRASP-PR is worse (the higher the overlap value, the better is the result of the MAX-CMO problem, and the lower the value of RMSD, the better is the algorithm in terms os structure supreimposition) the RMSD value of

GRASP-PR is better (smaller) than the values found by the RB algorithm. Such ambiguity is already known and discussed since the work entitled “The structural alignment between two proteins: is there a unique answer?” (Godzik, 1996), justifying the use of heuristics capable of giving fast near-optimal solutions of meaningful alignments.

The superimpositions of this experiment are show in Figures 2-6, in which we can make a visual inspection of alignment. can make a visual inspection of alignment. A key observation made from these figures is that the GRASP-PR was able to align all the selected protein pairs, and the resultant superimpositions had a high similarity with the superimposition resultant from the alignment of the RB algorithm with much less effort of time and a simple strategy.

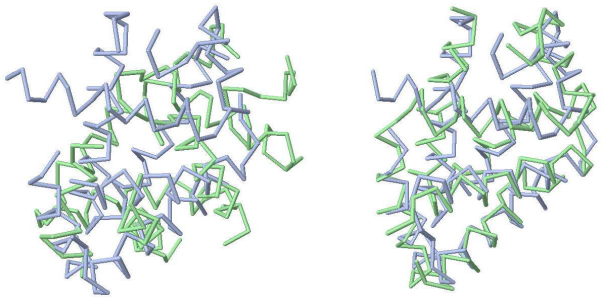

FIGURE 13 Protein backbones superimposition generated from: the GRASP-PR solution on the left side and the RB one on the right side. Instance 1 - 1ASH (Blue) and 1HLM (Green).

Figures of instances 2, 3, 4 and 5 show that the alignment is identical to the naked eye for the two algorithms. For instances 4 and 5, this high similarity was expected, since both algorithms reached the exact value of overlaps. But for instance 2, even without reaching the optimal value of overlap, the GRASP-PR showed an alignment very similar to the RB algorithm, in addition to obtaining a better value of RMSD. In this figure 1, alignment of GRASP-PR differs somewhat

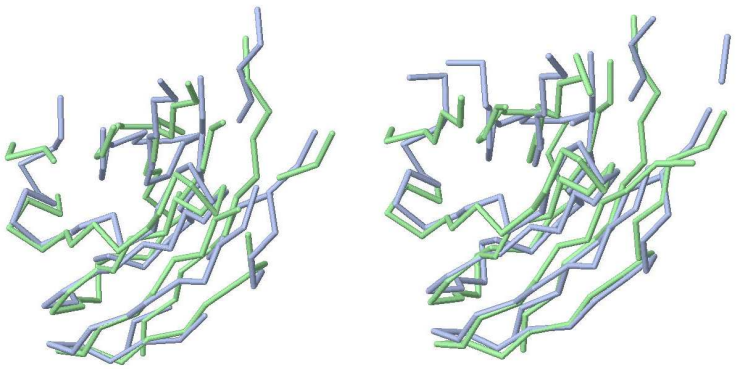

FIGURE 14 Protein backbones superimposition generated from: the GRASP-PR solution on the left side and the RB one on the right side. Instance 2 - 1QFO (Blue) and1NEU (Green).

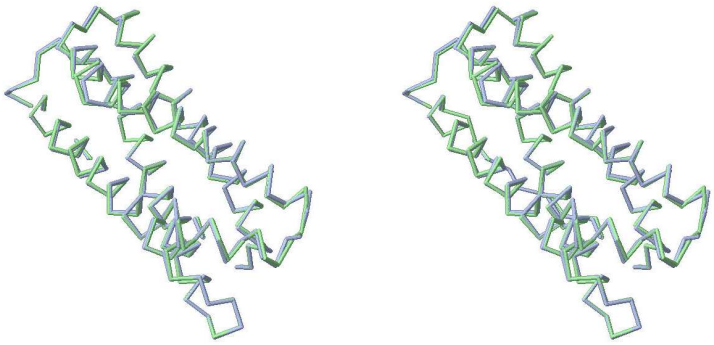

FIGURE 15 Protein backbones superimposition generated from: the GRASP-PR solution on the left side and the RB one on the right side. Instance 3 - 1RCD (Blue) and 1IER (Green).

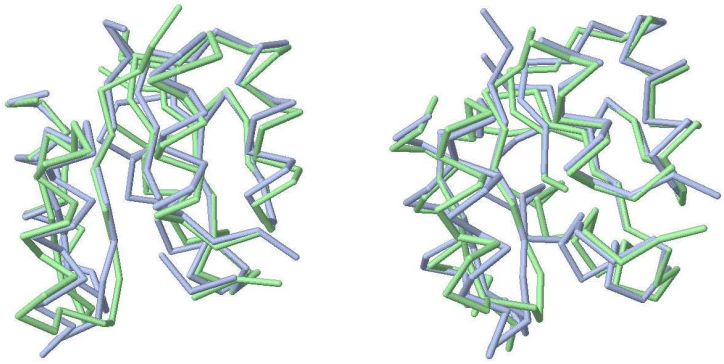

FIGURE 16 Protein backbones superimposition generated from: the GRASP-PR solution on the left side and the RB one on the right side. Instance 4 - 4TMT (Blue) and 1QMPB (Green).

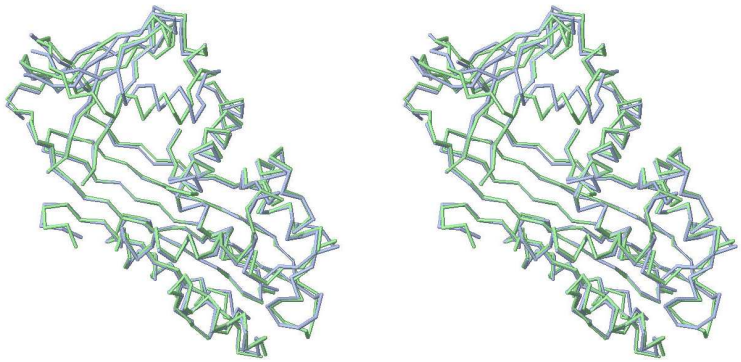

FIGURE 17 Protein backbones superimposition generated from: the GRASP-PR solution on the left side and the RB one on the right side. Instance 5 - 2ACH (Blue) and 7API (Green).

from the alignment of the RB algorithm, but both alignments seem to be significant as the difference in the RMSD between the algorithms value is very low.

The study performed in this dataset shows that our strategy can replicate the results obtained using exact methods but with less computational effort and a simple strategy. Moreover, this experiment illustrates that non-exact MAX-CMO values may have solutions as meaningful as the exact ones. Both elements are important results *per se*. We should mention that the all experiments done in this final chapter can be done through Biocomp-Server described in Chapter 2.

6 CONCLUDING REMARKS

In this work, we tested a straight and simple GRASP implementation with Path-Relinking for the MAX-CMO problem, which obtains encouraging results. Computational results demonstrate that the heuristic is a well-suited approach for the MAX-CMOP, and comparisons with other successful heuristics from literature show that the proposed heuristic produces results very competitive. GRASP-PR obtained results that were very well applied to real problems using less computational effort than exact algorithms. Moreover, we mention that all experiments conducted in this paper can be reproduced using the Goic-Biocomp server at `http://goic.dcc.ufla.br/Biocomp`.

7 REFERENCES

BARTOLI, L.; CAPRIOTTI, E.; FARISELLI, P.; MARTELLI, P. L.; R., C. The pros and cons of predicting protein contact maps. **Methods in Molecular Biology**, Totowa, v. 413, p. 199–217, Feb. 2008.

BERMAN, H. M.; WESTBROOK, J.; FENG, Z.; GILLILAND, G.; BHAT, T. N.; WEISSIG, H.; SHINDYALOV, I. N.; BOURNE, P. E. The protein data bank. **Nucleic Acids Research**, Oxford, v. 28, n. 1, p. 235–42., Jan. 2000.

CAPRARA, A.; CARR, R.; ISTRAIL, S.; LANCIA, G.; WALENZ, B. 1001 optimal pdb structure alignments: integer programming methods for finding the maximum contact map overlap. **Journal of Computational Biology**, New York, v. 11, n. 1, p. 27–52, Jan. 2004.

CAPRARA, A.; LANCIA, G. Structural alignment of large-size proteins via Lagrangian relaxation. In: *ANNUAL CONFERENCE ON RESEARCH IN COMPUTATIONAL MOLECULAR BIOLOGY*, 6., 2002, Washingthon. **Proceedings of the Sixth Annual International Conference on Computational Biology**. Washingthon: ACM, 2002. p. 100-108.

CARR, B.; HART, W.; KRASNOGOR, N.; HIRST, J.; BURKE, E.; SMITH, J. Alignment of protein structures with a memetic evolutionary algorithm. In: *GENETIC AND EVOLUTIONARY COMPUTATION CONFERENCE*, 2002, New York. **Proceedings of the Genetic and Evolutionary Computation Conference**, New York: Morgan, 2002. p. 1027-1034.

CHEW, L. P.; KEDEM, K. Finding the consensus shape for a protein family. In: *Proceedings of the 18th Annual Symposium on Computational Geometry*, 18., 2002, Barcelona. **Proceedings of the 18th Annual Symposium on Computational Geometry** Barcelona: ACM, 2002. p. 64-73.

COCK, P. J.; ANTAO, T.; CHANG, J. T.; CHAPMAN, B. A.; COX, C. J.; DALKE, A.; FRIEDBERG, I.; HAMELRYCK, T.; KAUFF, F.; WILCZYNSKI, B.; HOON, M. J. L. de. Biopython: freely available python tools for computational molecular biology and bioinformatics. **Bioinformatics**, Oxford, v. 25, n. 11, p. 1422–1423, Mar. 2009.

DIETMANN, S.; PARK, J.; NOTREDAME, C.; HEGER, A.; LAPPE, M.; HOLM, L. A fully automatic evolutionary classification of protein folds: dali domain dictionary version 3. **Nucleic Acids Research**, Oxford, v. 29, n. 1, p. 55–57, Jan. 2001.

FEO, T.; RESENDE, M.; SMITH, S. A greedy randomized adaptive search procedure for maximum independent set. **Operations Research**, Baltimore, v. 42, n. 5, p. 860–878, Sept./Oct. 1994.

FEO, T. A.; RESENDE, M. G. Greedy randomized adaptive search procedures. **Journal of Global Optimization**, Dordrecht, v. 6, n. 2, p. 109–133, Mar. 1995.

GLOVER, F. Tabu search and adaptive memory programming: advances, applications, and challenges. In: BARR, R. S.; HELGASON, R. V.; KENNINGTON, J. L. (Ed.). **Interfaces in computer science and operations research**: advances in metaheuristics, optimization, and stochastic modeling technologies. Boston: Kluwer Academic, 1996. p. 1–75.

GODZIK, A. The structural alignment between two proteins: is there a unique answer? **Protein Science**, Cold Spring Harbor, v. 5, n. 7, p. 1325–1338, July 1996.

GODZIK, A.; KOLINSKI, A.; SKOLNICK, J. Topology fingerprint approach to the inverse protein folding problem. **Journal of Molecular Biology**, London, v. 227, n. 1, p. 227–238, Sept. 1992.

GOLDMAN, D.; ISTRAIL, S.; PAPADIMITRIOU, C. Algorithmic aspects of protein structure similarity. In: ANNUAL SYMPOSIUM ON FOUNDATIONS OF COMPUTER SCIENCE, 40., 1999, New York. **Proceedings of 40th Annual Symposium on Foundations of Computer Science**, New York: IEEE Computer Society, 1999. p. 512-521.

GOLDSMITH-FISCHMAN, S.; HONIG, B. Structural genomics: computational methods for structure analysis. **Protein Science**, Cold Spring Harbor, v. 12, n. 9, p. 1813–1821, Sept. 2003.

GREENBERG, H. J.; HART, W. E.; LANCIA, G. Opportunities for combinatorial optimization in computational biology. **Informs Journal on Computing**, Linthicum, v. 16, n. 3, p. 211–231, 2004.

HO, H. K.; KUIPER, M. J.; KOTAGIRI, R. Pconpy–a python module for generating 2d protein maps. **Bioinformatics**, Oxford, v. 24, n. 24, p. 2934–2935, Oct. 2008.

KRASNOGOR, N.; LANCIA, G.; ZEMLA, A.; HART, W. E.; CARR, R. D.; HIRST, J.; BURKE, E. A Comparison of Computational Methods for the Maximum Contact Map Overlap of Protein Pairs. 2003. Available at: < `http://citeseerx.ist.psu.edu/viewdoc/summary?doi=10.1.1.3.4526` >. Accessed: 3 dez. 2009.

LAGUNA, M.; MARTÍ, R. Grasp and path relinking for 2-layer straight line crossing minimization. **Informs** Journal on Computing, Linthicum, v. 11, n. 1, p. 44–52, 1999.

LANCIA, G.; CARR, R.; WALENZ, B.; ISTRAIL, S. 101 optimal pdb structure alignments: A branch and cut algorithm for the maximum contact map overlap problem. In: *ANNUAL CONFERENCE ON RESEARCH IN COMPUTATIONAL MOLECULAR BIOLOGY*, 5., 2001, New York. **Proceedings of the Fifth Annual Conference on Research in Computational Molecular Biology**, New York: ACM, 2001. p. 193-202.

LANCIA, G.; ISTRAIL, S. Protein structure comparison: algorithms and applications. In: GUERRA, C.; ISTRAIL, S. (Ed.). **Protein structure analysis and design**: lecture notes in bioinformatics. Berlin: Springer, 2004. v. 266, p. 1–33.

LELUK, J.; KONIECZNY, L.; ROTERMAN, I. Search for structural similarity in proteins. **Bioinformatics**, Oxford, v. 19, n. 1, p. 117–124, Jan. 2003.

MATEUS, G.; RESENDE, M.; SILVA, R. GRASP with path-relinking for the generalized quadratic assignment problem. 2009. Available at: < `http://www.optimization-online.org/DB_FILE/2009/01/2186.pdf` >. Accessed: 23 nov. 2009.

MATSUMOTO, M.; NISHIMURA, T. Mersenne twister: a 623-dimensionally equidistributed uniform pseudo-random number generator. **ACM Transactions on Modeling and Computer Simulation**: a publication of the association for computing machinery, New York, v. 8, n. 1, p. 3–30, Jan. 1998.

MURZIN, A. G.; BRENNER, S. E.; HUBBARD, T.; CHOTHIA, C. Scop: a structural classification of proteins database for the investigation of sequences and structures. **Journal of Molecular Biology**, London, v. 247, n. 4, p. 536–540, Apr. 1995.

PELTA, D. A.; GONZALEZ, J. R.; VEGA, M. M. A simple and fast heuristic for protein structure comparison. **BMC Bioinformatics**, London, v. 9, p. 161–177, Mar. 2008.

RESENDE, M.; RIBEIRO, C. Greedy randomized adaptive search procedures. In: GLOVER, F.; KOCHENBERGER, G. (Ed.). **Handbook of Metaheuristics**. Dordrecht: Kluwer Academic, 2003. p. 219–249.

RESENDE, M.; RIBEIRO, C. Grasp with path-relinking: recent advances and applications. In: IBARAKI, T.; NONOBE, K.; YAGIURA, M. (Ed.). **Metaheuristics**: progress as real problem solvers. New York: Springer, 2005. p. 29–63.

WESTBROOK, J.; FENG, Z.; CHEN, L.; YANG, H.; BERMAN, H. M. The protein data bank and structural genomics. **Nucleic Acids Research**, Oxford, v. 31, n. 1, p. 489–491, Jan. 2003.

WIEMAN, H.; TONDEL, K.; ANDERSSEN, E.; DRABLOS, F. Homology-based modelling of targets for rational drug design. **Mini-Reviews in Medicinal Chemistry**, Hilversum, v. 4, n. 7, p. 793–804, Sept. 2004.

WOLFON, H. J.; SHATSKY, M.; SCHNEIDMAN-DUHOVNY, D.; DROR, O.; SHULMAN-PELEG, A.; MA, B.; NUSSINOV, R. From structure to function: methods and applications. **Current Protein and Peptide Science**, Amsterdam, v. 6, n. 2, p. 171–183, Apr. 2005.

XIE, W.; SAHINIDIS, N. V. A branch-and-reduce algorithm for the contact map overlap problem. In: *INTERNATIONAL CONFERENCE ON RESEARCH IN COMPUTATIONAL MOLECULAR BIOLOGY*, 10., 2006, Venice. **Proceedings of RECOMB of Lecture Notes in Bioinformatics** Berlin: Springer, 2006. p. 516–529. (RECOMB of Lecture Notes in Bioinformatics).

XIE, W.; SAHINIDIS, N. V. A reduction-based exact algorithm for the contact map overlap problem. **Journal of Computational Biology**, New York, v. 14, n. 5, p. 637–654, June 2007.

CHAPTER 3

GOIC-BIOCOMP: A WEB-BASED TOOL FOR PROTEIN ALIGNMENT

1 ABSTRACT

Protein structure comparison and clustering are key problems in bioinformatics. An available and efficient alternative to perform protein structural comparison is to align the contact maps of protein pairs. This approach can be formulated as a well known mathematical problem called Maximum Contact Map Overlap Problem (MAX-CMO). Tools are still required to solve the problem by using algorithms that obtain good quality solutions using less computational and time resources. This paper presents a web-based tool for protein structure alignment based on the greedy randomized adaptive search procedure with path-relinking (GRASP-PR) for MAX-CMO problem. Experiments can be performed via web comparing the GRASP-PR heuristic with other algorithms from literature. The tool is available: `http://goic.dcc.ufla.br/Biocomp`.

2 RESUMO

Comparação de estruturas de proteínas é um problema chave em bioinformática. Uma alternativa eficiente disponível para realizar a comparação estrutural de proteínas é alinhar os mapas de contatos de pares de proteínas. Essa abordagem pode ser formulada como um problema matemático bem conhecido chamado Maximum Contact Map Overlap (MAX-CMO). Ferramentas que resolvem esse problema usando algoritmos que obtêm soluções de boa qualidade usando menos recursos computacionais e tempo ainda são requeridos. Esse artigo apresenta uma ferramenta web para o alinhamento estrutural de proteínas baseado na heurística greedy randomized adaptive search procedure com path-relinking (GRASP-PR) para o MAX-CMO. Experimentos podem ser realizados via web comparando a heurística GRASP-PR com outros algoritmos da literatura. A ferramenta é disponível em `http://goic.dcc.ufla.br/Biocomp`.

3 GRASP WITH PATH-RELINKING FOR MAX-CMO

Recently, the growth of the Protein Data Bank (PDB) (Berman et al., 2000) has been accelerated by a large scale structure determination project, called *structural genomics* (Westbrook et al., 2003). As a result, fast and efficient algorithms for protein structure comparison have become more important to take advantage of the huge amount of structural data.

One promising way of accomplishing the structural alignment is to evaluate the alignment of their contact maps, which are used to represent the distances between every pair of residues in a three-dimensional protein structure.

In the graph representation, the contact map $G = (V, E)$ is a graph with a set of nodes V corresponding to the sequence of residues and a set of edges E corresponding to the edges for each pair of non-consecutive residues whose distance is below a given threshold.

Given two contact maps $G_A = (V_A, E_A)$ and $G_B = (V_B, E_B)$ such that $|V_A| = n$ and $|V_B| = m$, the CONTACT MAP OVERLAP PROBLEM (Goldman et al., 1999) is to find two subsets $S_A \subseteq V_A$ and $S_B \subseteq V_B$ with $|S_A| = |S_B|$ and an order preserving bijection f between S_A and S_B such that the cardinality of the *overlap set*

$$\mathcal{L}(S_A, S_B, f) = \{(u, v) \in E_A \ : \ u, v \in S_A, \ (f(u), f(v)) \in E_B\}$$

is maximized. A solution (S_A, S_B, f) for the contact map overlap problem can be represented as an assignment vector p of size n such that

$$p_u = \begin{cases} v & \text{if } (u, v) \in \mathcal{L}(S_A, S_B, f) \\ \texttt{nil} & \text{otherwise.} \end{cases}$$

Algorithm 1 shows pseudo-code for the GRASP (Feo & Resende, 1995) with path-relinking (Glover, 1996) heuristic for the MAX-CMO problem. The algorithm takes as input two contact maps C^A and C^B of proteins A and B, with n and m residues ($m > n$), respectively. It outputs an array p^* of length n, with $p_i^* = \texttt{nil}$, if node $i \in C^A$ representing residue $i \in A$ is not aligned, and $p_i^* = j$, if node $i \in C^A$ is aligned with node $j \in C^B$.

After initializing the elite set P as empty, the GRASP with path-relinking iterations are computed until a stopping criterion is satisfied. This criterion could be, for example, a maximum number of iterations, a target solution quality, or a maximum number of iterations without improvement. In all iterations, a greedy randomized solution p is generated and tentatively improved with a local search.

If the elite set P is empty, solution p is added to it. If the elite set is not empty, then while it is not full, solution p is added to it if it is sufficiently different from the solutions already in the elite set. In order to define the term "sufficiently different" more precisely, let $\Delta(p, q)$ denote the number of assignments in p that are different from those in q. For a given level of difference δ, we say p is sufficiently different from all elite solutions in P if $\Delta(p, q) > \delta$ for all $q \in P$, which we indicate with the notation $p \not\approx P$.

If the elite set P is full, then path-relinking is applied between p and some elite solution q randomly chosen from P, resulting in solution r. Next, r is updated by a local minimum in its neighborhood. If r is the best solution found so far, then it replaces t, the solution most similar to it. Otherwise, if r is better than the worst solution in P and $r \not\approx P$, then it replaces t, the solution most similar to it.

Several exact algorithms as well as heuristics have been since proposed for MAX-CMO problem. In addition to GRASP-PR heuristic, BIOCOMP web tool provides some algorithms from literature as follows. A Lagrangian relaxation ap-

proach proposed by Caprara & Lancia (2002), where the optimal Lagrange multipliers are found by subgradient optimization. A dynamic programming as tool to design a branch-and-bound algorithm with several reduction techniques to eliminate inferior residue-residue pairs early in the search procedure proposed as a reduction based exact algorithm by Xie & Sahinidis (2007). A multi-start variable neighborhood search heuristic for solving MAX-CMO developed by Pelta et al. (2008).

procedure GRASP+PR-CMOP
  Input: C^A, C^B
  Output: solution p^*
  $P \leftarrow \emptyset$;
  while *stopping criterion not satisfied* **do**
    $p \leftarrow$ `GreedyRandomized`$(\cdot)$;
    $p \leftarrow$ `LocalSearch`(p);
    if P *is full* **then**
      Randomly select a solution $q \in P$;
      $r \leftarrow$ `PathRelinking`(p, q);
      $r \leftarrow$ `LocalSearch`(r);
      if $c(r) > \max\{c(s) : \ s \in P\}$ **then**
        $t \leftarrow \mathbf{argmin}\{\Delta(r, s) : \ s \in P\}$;
        $P \leftarrow P \cup \{r\} \setminus \{t\}$;
      else if $c(r) > \min\{c(s) : \ s \in P\}$ **and** $r \not\approx P$ **then**
        $t \leftarrow \mathbf{argmin}\{\Delta(r, s) : \ s \in P : \ c(s) < c(r)\}$;
        $P \leftarrow P \cup \{r\} \setminus \{t\}$;
      end
    else
      if $P = \emptyset$ **then**
        $P \leftarrow \{p\}$;
      else if $p \not\approx P$ **then**
        $P \leftarrow P \cup \{p\}$;
      end
    end
  end
  return $p^* = \mathbf{argmax}\{c(s) : \ s \in P\}$;

Algorithm 1: GRASP-PR for MAX-CMO algorithm.

4 GOIC-BIOCOMP SERVER

Goic-Biocomp server (Figure 1) takes as input the selected algorithm for the MAX-CMO problem and the PDB files (Westbrook et al., 2003) corresponding to the proteins to be aligned. The protein contact maps used as input for the algorithm are generated from the input PDB files. The algorithm outputs the residue alignment and the cardinality of the overlap set. Depending on the comparison approach, a different set of information are reported in the output web page. In pairwise comparison approach, besides the algorithms results, we have the binary and real two-dimensional matrix representation of the contact maps and also the superimposed proteins plot. While these matrixes are generated by `PConPy` tool (Ho et al., 2008) from protein PDB files, the superimposed PDB plots are created by `JMOL` tool. (Jmol, 2009) takes as input superimposed PDB files created by BioPython tool from the residue alignment. `Biopython` (Cock et al., 2009) is also responsible to compute the *root mean square deviation* (RMSD), the average distance between the backbones of superimposed proteins.

In multiple comparison approach, three or more proteins are compared all-against-all through the pairwise approach. The result is a symmetric two-dimensional matrix having as distance metric the cardinality of the overlap set of each pairwise structure alignment. This matrix is normalized according to two normalization schemes reported by (Lancia & Istrail, 2004) and (Xie & Sahinidis, 2004). Next, the normalized matrix is used as input for three clustering methods (Everitt & Dunn, 1992): single, complete and average linkage clustering. At the end, the clustering results are plotted as dendograms using R statistical tool (R Development Core Team, 2005).

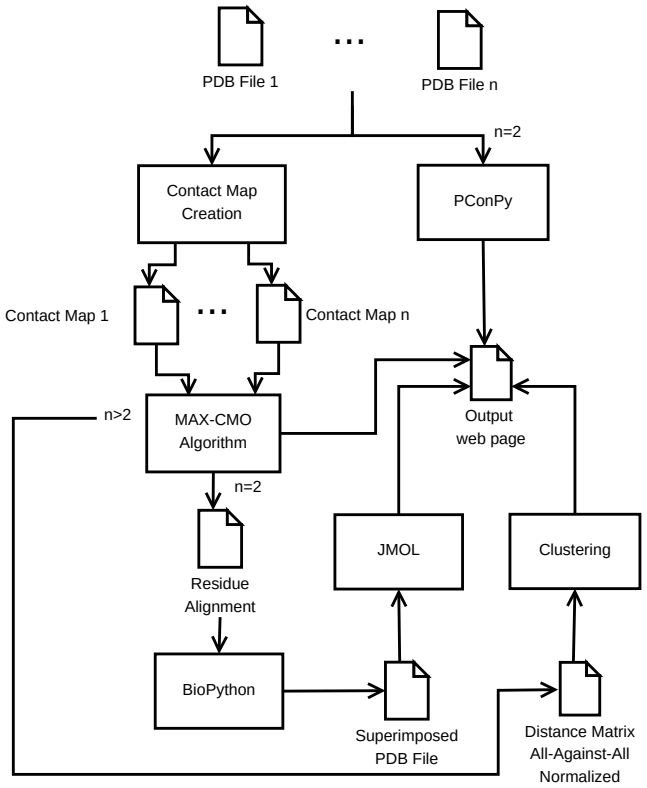

FIGURE 1 Goic-Biocomp architecture

Acknowledgement: The authors wish to thank Alberto Caprara, Giuseppe Lancia, Juan R Gonzalez and Nick Sahinidis for the programs provided and the authorization to make them available on the site. The AT&T Labs Research, Florham Park, New Jersey, USA. Support for this effort was provided through National Council of Scientific and Technological Development (CNPq), Brazil and Fundação à Pesquisa do Estado de Minas Gerais (FAPEMIG), Brazil.

5 REFERENCES

BERMAN, H. M.; WESTBROOK, J.; FENG, Z.; GILLILAND, G.; BHAT, T. N.; WEISSIG, H.; SHINDYALOV, I. N.; BOURNE, P. E. The protein data bank. **Nucleic Acids Research**, Oxford, v. 28, n. 1, p. 235–242., Jan. 2000.

CAPRARA, A.; LANCIA, G. Structural alignment of large-size proteins via Lagrangian relaxation. In: *ANNUAL CONFERENCE ON RESEARCH IN COMPUTATIONAL MOLECULAR BIOLOGY*, 6., 2002, Washingthon. **Proceedings of the Sixth Annual International Conference on Computational Biology**, Washingthon: ACM, 2002. p. 100-108.

COCK, P.; ANTAO, T.; CHANG, J.; CHAPMAN, B.; COX, C.; DALKE, A.; FRIEDBERG, I.; HAMELRYCK, T.; KAUFF, F.; WILCZYNSKI, B.; HOON, M. J. L. de. Biopython: freely available python tools for computational molecular biology and bioinformatics. **Bioinformatics**, Oxford, v. 25, n. 11, p. 1422–1423, Mar. 2009.

EVERITT, B. S.; DUNN, G. **Applied Multivariate Data Analysis**. New York: Oxford University, 1992.

FEO, T. A.; RESENDE, M. G. Greedy randomized adaptive search procedures. **Journal of Global Optimization**, Dordrecht, v. 6, n. 2, p. 109–133, Mar. 1995.

GLOVER, F. Tabu search and adaptive memory programming: advances, applications, and challenges. In: BARR, R. S.; HELGASON, R. V.; KENNINGTON, J. L. (Ed.). **Interfaces in computer science and operations research**: advances in metaheuristics, optimization, and stochastic modeling technologies. Boston: Kluwer Academic, 1996. p. 1–75.

GOLDMAN, D.; ISTRAIL, S.; PAPADIMITRIOU, C. Algorithmic aspects of protein structure similarity. In: *ANNUAL SYMPOSIUM ON FOUNDATIONS OF COMPUTER SCIENCE*, 40., 1999, New York. **Proceedings of 40th Annual Symposium on Foundations of Computer Science**, New York: IEEE Computer Society, 1999. p. 512-521.

HO, H. K.; KUIPER, M. J.; KOTAGIRI, R. Pconpy–a python module for generating 2d protein maps. **Bioinformatics**, Oxford, v. 24, n. 24, p. 2934–2935, Oct. 2008.

JMOL. Jmol: an open-source Java viewer for chemical structures in 3D. 2009. Available at: <http://jmol.sourceforge.net/>. Accessed: 19 nov. 2009.

LANCIA, G.; ISTRAIL, S. Protein structure comparison: algorithms and applications. In: GUERRA, C.; ISTRAIL, S. (Ed.). **Protein structure analysis and design**: lecture notes in bioinformatics. Berlin: Springer, 2004. v. 266, p. 1–33.

PELTA, D. A.; GONZALEZ, J. R.; VEGA, M. M. A simple and fast heuristic for protein structure comparison. **BMC Bioinformatics**, London, v. 9, p. 161–177, Mar. 2008.

R DEVELOPMENT CORE TEAM. **R**: a language and environment for statistical computing. Viena: R Foundation for Statistical Computing, 2004. Available at: <http://www.R-project.org>. Accessed : 20 dez. 2009.

WESTBROOK, J.; FENG, Z.; CHEN, L.; YANG, H.; BERMAN, H. M. The protein data bank and structural genomics. **Nucleic Acids Research**, Oxford, v. 31, n. 1, p. 489–491, Jan. 2003.

XIE, W.; SAHINIDIS, N. V. A branch-and-reduce algorithm for the contact map overlap problem. In: *INTERNATIONAL CONFERENCE ON RESEARCH IN COMPUTATIONAL MOLECULAR BIOLOGY*, 10., 2006, Venice. **Proceedings of RECOMB of Lecture Notes in Bioinformatics** Berlin: Springer, 2006. p. 516–529. (RECOMB of Lecture Notes in Bioinformatics).

XIE, W.; SAHINIDIS, N. V. A reduction-based exact algorithm for the contact map overlap problem. **Journal of Computational Biology**, New York, v. 14, n. 5, p. 637–654, June 2007.

CHAPTER 4

SUMMARY, GENERAL CONCLUSIONS AND FUTURE WORK

1 ABSTRACT

The final chapter contains the summary, general conclusions and outlines the possibilities for future work with the GRASP-PR algorithm presented in Chapter 2 and the Goic-Biocomp web tool described in Chapter 3.

2 RESUMO

O último capítulo contém o resumo, as conclusões gerais e descreve as possibilidades de trabalho futuro com o algoritmo GRASP-PR apresentado no capítulo 2 e a ferramenta web Goic-Biocomp descrita no Capítulo 3.

3 SUMMARY AND GENERAL CONCLUSION AND FUTURE WORK

Protein structure comparison is one of the most important problems in bioinformatics (see Chapter 1, Section 2). One approach for solving this problem is to first, extract protein binary contact maps from the protein tertiary structure (see Chapter 1, Section 1), and next, align these contact maps. In order to guide the design and development of a new algorithm to solve this problem, we used the Maximum Contact Map Overlap (MAX-CMO), one of the most common mathematical statements of the contact map alignment problem. Our purpose is based on the hybridization of two promising heuristics, called Greedy Random Adaptive Search Procedure with Path-Relinking (GRASP-PR) for the MAX-CMO.

Initially, we aimed to validate our proposal by comparing the results obtained by other popular algorithms described in the literature that solve the MAX-CMO problem. Based on the performed comparisons and analysis, we can observe that the GRASP-PR is very competitive when compared against some of the most successful algorithms: the Variable Neighborhood Search heuristic and the Lagrangian Relaxation algorithm. In addition, from an optimization point of view, we can mention at least two ways to obtain further improvements to our propose (Chapter 2, Section 2): a) by trying more specialized Greedy randomized construction procedures and b) by better tuning the parameters' values chosen.

An important element in several bioinformatics problems is the relation between the optimum value of the objective function and the biological relevance of the corresponding solution. In protein structure comparison, we should remember that we are dealing with a mathematical model that captures some aspects of the biological problem, being possible to measure protein structure similarity in several ways. For example, up to 37 measures are reviewed in (May, 1999).

Then, in a second moment, we aimed at investigating whether our heuristic

provides biologically meaningful alignments for practical instances; further investigating whether GRASP-PR can replicate the results obtained by applying exact methods with less computational effort. In order to accomplish this, we used three different assessment criteria for the algorithms: the overlap value, RMSD value and a visual inspection of the superimposition of the structures guided by the correspondence between residues of two proteins obtained by the MAX-CMO. We showed that our strategy can replicate the results obtained using exact methods but with less computational on practical instances. Furthermore, we observed that not always the different similarity measures and criteria for evaluating structural alignment algorithms agree with each other, a question much discussed since 1996 in the work entitled "The structural alignment between two proteins: is there a unique answer?" (Godzik, 1996). In this sense, a promising strategy would be to combine two of the most used similarity metrics in an attempt to reshape the MAX-CMO problem with a multi-objective function: minimize the RMSD and to maximize the number of overlaps.

Besides obtaining the highest overlap values, it is also critical to develop strategies able to obtain a proper similarity ranking of proteins. Our experiments showed that in terms of SCOP's family the (normalized) overlap values given by the GRASP-PR seemed to be good enough to capture the similarity.

After the GRASP-PR algorithm was implemented and validated, we built an interface that allows easy use of MAX-CMO algorithms in order to perform the pairwise structural alignment or structural clustering of proteins. This web interface is available at `http://goic.dcc.ufla.br` and we call it Goic-Biocomp web tool (Chapter 3). Goic-Biocomp server produces up to six kinds of output when the task of pairwise structural alignment is requested: (i) the distance map plots; (ii) the contact map plots; (iii) a PDB file containing the coordinates of the

superimposed molecules; (iv) a sequence alignment corresponding to the equivalent residues found by the MAX-CMO; (v) an RMSD report that contains the calculated RMSD values (in Angstroms) between the superimposed molecules; (vi) a JMol (Jmol, 2009) applet view of the superimposed molecules. For the structural clustering, the Goic-Biocomp server produces the dendogram as output.

In summary, Goic-Biocomp web tool provides a simple-to-use, web-accessible approach to performing the structural pairwise alignment and the structural clustering, via MAX-CMO using different successful algorithms reported in literature, allowing several studies on protein structures with different purposes - The interested reader is referred to (Wolfon et al., 2005) for a detailed description of methods and applications for the determination of protein function.

4 REFERENCES

GODZIK, A. The structural alignment between two proteins: is there a unique answer? **Protein Science**, Cold Spring Harbor, v. 5, n. 7, p. 1325–1338, July 1996.

JMOL. Jmol: an open-source Java viewer for chemical structures in 3D. 2009. Available at: <`http://jmol.sourceforge.net/`>. Accessed: 19 nov. 2009.

MAY, A. Towards More Meaningful Hierarchical classification of aminoacids scoring matrices. **Protein Engineering**, Oxford, v. 12, n. 9, p. 707-712, Sept. 1999.

WOLFON, H. J.; SHATSKY, M.; SCHNEIDMAN-DUHOVNY, D.; DROR, O.; SHULMAN-PELEG, A.; MA, B.; NUSSINOV, R. From structure to function: methods and applications. **Current Protein and Peptide Science**, Amsterdam, v. 6, n. 2, p. 171–183, Apr. 2005.